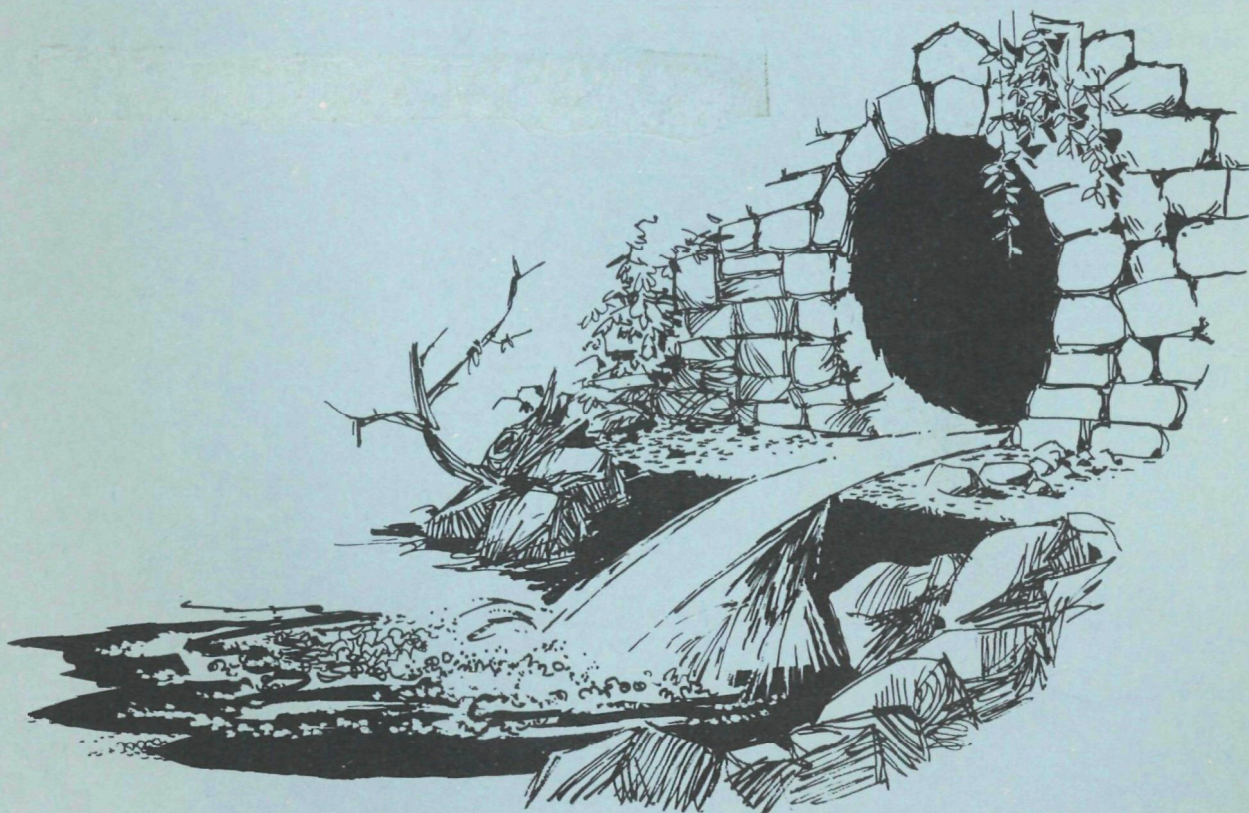


# Hydraulics of Long Vertical Conduits and Associated Cavitation



## WATER POLLUTION CONTROL RESEARCH SERIES

The Water Pollution Control Research Reports describe the results and progress in the control and abatement of pollution of our Nation's waters. They provide a central source of information on the research, development and demonstration activities of the Water Quality Office of the Environmental Protection Agency, through in-house research and grants and contracts with the Federal, State and local agencies, research institutions, and industrial organizations.

Previously issued reports on the Storm and Combined Sewer Pollution Control Program:

11023 FDB 09/70	Chemical Treatment of Combined Sewer Overflows
11024 FKJ 10/70	In-Sewer Fixed Screening of Combined Sewer Overflows
11023 --- 12/70	Urban Storm Runoff and Combined Sewer Overflow Pollution
11023 DZF 06/70	Ultrasonic Filtration of Combined Sewer Overflows
11020 FAQ 03/71	Dispatching System for Control of Combined Sewer Losses
11022 EFF 12/70	Prevention and Correction of Excessive Infiltration and Inflow into Sewer Systems - A Manual of Practice
11022 EFF 01/71	Control of Infiltration and Inflow into Sewer Systems
11022 DPP 10/70	Combined Sewer Temporary Underwater Storage Facility
11024 EQG 03/71	Storm Water Problems and Control in Sanitary Sewers - Oakland and Berkeley, California
11020 FAL 03/71	Evaluation of Storm Standby Tanks - Columbus, Ohio
11024 DOC 07/71	Storm Water Management Model, Volume I - Final Report
11024 DOC 08/71	Storm Water Management Model, Volume II - Verification and Testing
11024 DOC 09/71	Storm Water Management Model, Volume III - User's Manual
11024 DOC 10/71	Storm Water Management Model, Volume IV - Program Listing
11040 GKK 06/70	Environmental Impact of Highway Deicing
11024 DQU 10/70	Urban Runoff Characteristics
11024 EQE 06/71	Impregnation of Concrete Pipe
11024 EJC 10/70	Selected Urban Storm Water Runoff Abstracts, First Quarterly Issue
11024 EJC 01/71	Selected Urban Storm Water Runoff Abstracts, Second Quarterly Issue
11024 FJE 04/71	Selected Urban Storm Water Runoff Abstracts, Third Quarterly Issue
11024 FJE 07/71	Selected Urban Storm Water Runoff Abstracts, July 1971 - June 1971
11023 FDD 07/71	Demonstration of Rotary Screening for Combined Sewer Overflows
11024 FLY 06/71	Heat Shrinkable Tubing as Sewer Pipe Joints

To be continued on inside back cover....

HYDRAULICS OF LONG VERTICAL CONDUITS  
AND ASSOCIATED CAVITATION

by

St. Anthony Falls Hydraulic Laboratory  
University of Minnesota  
Minneapolis, Minnesota 55455

for the

ENVIRONMENTAL PROTECTION AGENCY

Project #11034 FLU  
Contract # 14-12-861

June 1971

### EPA Review Notice

This report has been reviewed by the Water Quality Office, EPA, and approved for publication. Approval does not signify that the contents necessarily reflect the views and policies of the Environmental Protection Agency, nor does mention of trade names or commercial products constitute endorsement or recommendation for use.



## ABSTRACT

Experimental studies have been undertaken to examine the flow in long vertical conduits with particular reference to the design of storm water drop shafts. A distinguishing characteristic of such flow is the potential cavitation regime. Its existence depends upon the design of the structure. The cavitation regime will develop when the conduit is sufficiently long and the head sufficiently large. It can also be generated at a lower head if a control valve is installed in the supply line so that the net head can be negative. The cavitation region consists of a rather finely divided mixture of water and water vapor at a constant cavitation pressure of about -32.0 ft of water throughout the region and for all discharges. The cavitation region terminates with a shock front whose location is also a function of the discharge. The concentration of vapor, while relatively constant throughout the cavitation region, decreases with increasing discharge.

If a small amount of air is introduced into the system, the cavitation region is eliminated, the pressure gradient is more uniform, and the flow consists of a uniform mixture of air and water.

This report was submitted in fulfillment of Project Number 11034 FLU, Contract EPA 14-12-861, under the sponsorship of the Water Quality Office, Environmental Protection Agency.

## CONTENTS

<u>Section</u>		<u>Page</u>
I	Conclusions	1
II	Recommendations	3
III	Introduction	5
IV	Experimental Apparatus	7
V	Experimental Results	11
	Cavitation Studies	11
	Air Injection	19
VI	Analysis of Data	27
VII	Head Discharge Rating Curves	37
	Transitional Flow	37
	Cavitation Flow	38
	Full Flow	42
	Flow Behavior Patterns	42
VIII	Acknowledgments	45
IX	References	47
X	Glossary of Symbols	49

## FIGURES

	<u>PAGE</u>
1 GEOMETRY OF DROP SHAFT	8
2 INLET TO VERTICAL CONDUIT SHOWING DISCHARGE MEASURING ORIFICE AND CONTROL VALVE	9
3 TRANSPARENT EXPERIMENTAL VERTICAL CONDUIT SHOWING PRESSURE GAGES AND INSTRUMENT PORTS	9
4 DETAIL OF INSTRUMENT PORTS FOR VAPOR CONCENTRATION MEASUREMENTS	10
5 TWO TYPES OF VAPOR-CONCENTRATION SENSORS: (a) PARALLEL PLATE PROBE; (b) NEEDLE PROBE	10
6 PRESSURE HEAD VARIATION ALONG SHAFT	12-13
7 PIEZOMETRIC HEAD ALONG SHAFT	14-15
8 VAPOR CONCENTRATIONS	16-17
9 SHOCK-FRONT ELEVATION vs DISCHARGE	18
10 VAPOR CONCENTRATION vs DISCHARGE	20
11 PIEZOMETRIC HEAD ALONG SHAFT WITH AIR INJECTION	21-22
12 AIR CONCENTRATIONS ALONG SHAFT	23
13 EFFECT OF AIR INJECTION ON WATER DISCHARGE	24
14 EFFECT OF AIR INJECTION ON SHAFT PRESSURE	25
15 SKETCH SHOWING FLOW REGIMES	28
16 SONIC VELOCITY vs AIR CONCENTRATION	29
17 COMPUTED AND OBSERVED SHOCK FRONT ELEVATIONS	33
18 COMPUTED AND OBSERVED VAPOR CONCENTRATIONS ABOVE SHOCK FRONT	35
19 THEORETICAL CURVES SHOWING SHOCK FRONT ELEVATION FOR VARYING PIPE LENGTHS	36
20 DISCHARGE RATING CURVES - Dia. = 5.0 in.	39
21 DISCHARGE RATING CURVES - Dia. = 1.0 ft	40
22 DISCHARGE RATING CURVES - Dia. = 2.0 ft	41

## SECTION I

### CONCLUSIONS

1. The cavitation regime in a long vertical conduit is a part of the complete head-discharge relationship. It will occur only if the head is large enough to prevent the insufflation of air or if there is a control valve in the inlet line. Its occurrence also depends on the size of the conduit.
2. The pattern for cavitating flow appears to be well defined and consists of the inlet region and an outlet full flow section connected by a relatively homogeneous mixture of water and water vapor flowing at a constant pressure of -31.75 ft of water for all discharges.
3. A shock front occurs at the downstream end of the cavitating region and causes an abrupt pressure increase.
4. The concentration of vapor in the cavitating region decreases with increasing discharge, and the shock front generated by the cavitating flow rises in elevation with increasing discharge, until the entire conduit runs full.
5. Small quantities of air injected into the system have very little effect on discharge and are very effective in eliminating the cavitation and the shock front. The mixture of air and water flows smoothly through the conduit.
6. It appears from the study that in terms of the complete discharge rating curve, the existence and the exploitation of a cavitation regime depend on design decisions. The present results can be used as a basis for preliminary design and for engineering feasibility studies.



## SECTION II

### RECOMMENDATIONS

This program was limited to a laboratory study of the cavitating phenomenon in a relatively short transparent vertical conduit. The equipment allowed the examination of many aspects of the cavitation process, such as pressure and vapor concentration distribution and the existence of the shock front, but the conduit was not long enough for an investigation of the effect of larger length-diameter ratios.

It is recommended that further measurements be made in a conduit both longer and of larger diameter under conditions approximating field installations.

In light of the present results it is recommended that additional laboratory measurements be made on a model equipped to transport larger discharges. These would include additional measurements on a similar model of greater length and smaller diameter.

Examination of the head-discharge rating curves indicates a wide range of possible transitional flow relationships depending upon the inlet geometry. It is recommended that this aspect be investigated in detail in order to define the head-discharge relationship more clearly for all practical design geometries.

## SECTION III

### INTRODUCTION

In large urban areas, polluttional considerations more and more require that surface runoff be treated before being discharged into streams. To facilitate the efficient and economical treatment of this polluted water it would be desirable to store the runoff temporarily so that the treatment process could operate over a period considerably longer in duration than the storm event and at a much lower rate of speed than that of the peak runoff. In some cases storage in large tunnels constructed in the rock some distance below the ground surface seems appropriate, and the surface water must be transported to these tunnels through vertical drop shafts which may be quite long. To minimize the size of the drop shaft, it obviously must run full when the discharge is maximal. Given this requirement, the size and spacing of the drop shafts for drainage of a particular area can be optimized by considering the local hydrology as well as the construction cost and the function of the drainage system. In some cases, the spacing of drop shafts may be governed by the requirement of minimum surface storage, as on a depressed roadway.

Drop shafts can be categorized as either atmospheric or subatmospheric pressure systems. In an atmospheric pressure system, the water simply falls down the shaft without completely filling the conduit, and the pressure is atmospheric throughout. In a subatmospheric pressure system the conduit flows full and the pressure thus decreases with increasing elevation. Since the conduit is flowing full, with a greater effective head, the velocities are greater than in an atmospheric pressure system, and hence the same discharge can be transported through a smaller conduit. However, since the velocities are larger and the pressure in certain sections is reduced to the cavitation pressure, special consideration must be given to the flow characteristics so that efficient operation can be obtained. With a knowledge of the flow pattern characteristics, the use of such drop shafts is governed by economics.

The purpose of the experimental program described herein was to examine and describe the hydraulic characteristics of flow in long vertical conduits with particular reference to the application of this phenomenon to storm water drop shafts. It was thought that the relationships developed through this research would provide a basis for the design of prototype structures. Because the vertical conduit was quite long, it was expected that the usual hydraulic relationships for conduit flow would not be directly applicable, since according to hydraulic theory, the pressure continually decreases as the elevation above the conduit outlet is increased with the conduit running full. For a conduit of sufficient length this pressure would decrease to the vapor pressure, and it was expected that cavitation in some form would occur. Therefore the first objective after the experimental apparatus had been fabricated was to visually examine the flow characteristics for various discharges and describe the phenomenon qualitatively. As was expected, when the discharge was sufficiently large to seal the lower portion of the

conduit, the flow in the upper part of the pipe where the pressure was at a minimum began to cavitate and appeared to be a milky mixture of water bubbles and water vapor flowing rapidly down the conduit. A crackling noise could be heard in the region immediately downstream of the control valve. At some elevation below the conduit inlet a shock front was created. The mixture was transformed back into solid water which filled the pipe and flowed at a much lower velocity through the remainder of the conduit. The flow below the shock front appeared to contain bubbles of air which might have been released from solution in the low-pressure region upstream of the shock front. The shock front was shifted bodily within the conduit when the discharge was changed. For the small discharges the shock front occurred at a relatively high elevation and tended to move downstream as the discharge increased until it reached a minimum elevation. With further increases in the discharge, the shock front developed at successively higher elevations until the conduit was running full and the shock front disappeared. On the basis of visual observation, provisions were made for measuring the several variables that appeared to have a bearing on the phenomenon. These included the discharge, the shock front elevation with respect to the conduit outlet, and the longitudinal distribution of pressure and vapor concentration. The measurements were made to provide detailed information about the nature of the flow and to serve as a basis for analytical relationships to describe the flow under these cavitating conditions which would aid in the design of drop shafts of other sizes and lengths.

In addition to those described above, some experiments were made to examine the effect of increasing the pressure in the conduit to a value above the cavitation pressure by injecting air into the system. This prevented cavitation and provided a uniform and more smoothly flowing air-water mixture. In such a system cavitation did not occur, and hence there was no likelihood of cavitation damage to the inside surface of the drop shaft. In these experiments, measured quantities of air were introduced into the system at the inlet, and the longitudinal distribution of pressure and air concentration was measured to delineate the characteristics of the mixture. The introduction of the air transformed the flow pattern from a cavitating flow with a shock front to a milky white mixture flowing smoothly through the system.

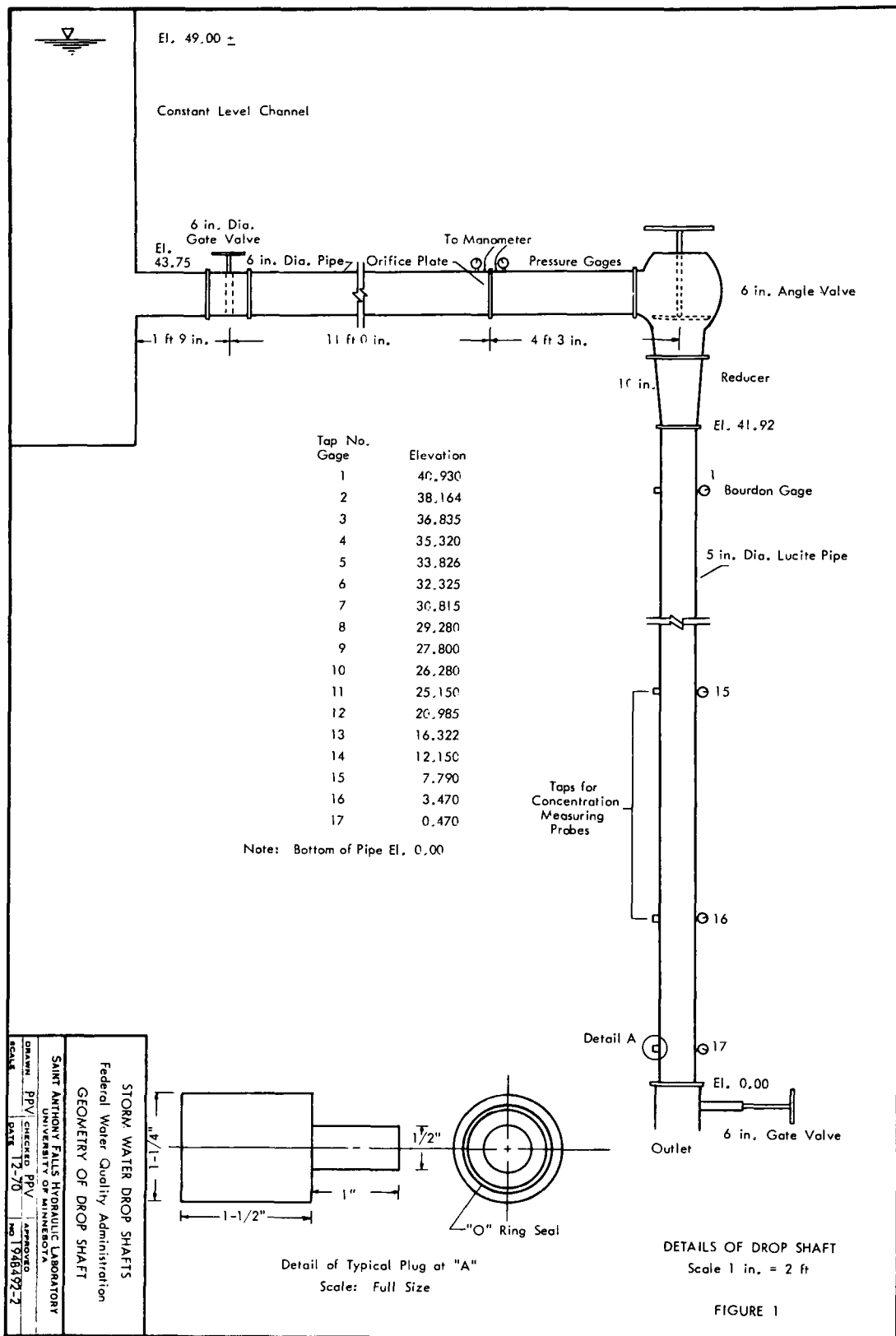
## SECTION IV

### EXPERIMENTAL APPARATUS

The hydraulic apparatus which was used for these experiments was a transparent vertical conduit 5 inches in diameter and approximately 43 feet high. This was the maximum height that could be obtained within the confines of the hydraulic laboratory without extensive modification of laboratory facilities. The model permitted the use of gravity flow from the Laboratory supply system. The water supply used in the experiments was obtained from the Mississippi River upstream of St. Anthony Falls. The discharge from the model was directed back to the river through the wasteway below the falls. In this way the full head available at the falls could be utilized for gravity flow through the system. The hydraulic model was open to the atmosphere at both the inlet and the outlet.

The discharge was controlled by a valve in the 6 inch pipe leading from the supply tank and was measured by means of a calibrated orifice. Figure 1 is a diagrammatic sketch of the apparatus and its appurtenances. Figure 2 is an overall view of the upstream portion of the drop shaft showing the supply pipe from the supply channel in the background. The flow through the conduit was controlled by the angle valve and measured by means of the orifice in the pipeline.

The drop shaft model was fitted with pressure gages and ports for the measurement of vapor concentration. These measurements were made with standard equipment or with instruments previously developed by the Laboratory. The pressures at various elevations along the conduit were measured by Bourdon gages fitted to piezometer taps drilled through the side of the conduit. Figure 3 shows a portion of the conduit and the pressure taps and gages for measuring the pressures. Ports for the insertion of the air concentration meter were fitted at various points along the pipe as shown in Fig. 4. Two types of vapor concentration instruments, shown in Fig. 5, were used. In one the vapor concentrations were determined by measuring the electrical resistance between two electrode surfaces. This is a function of the relative volume of water vapor moving between the electrodes. The other instrument measured vapor concentration at a point rather than taking the mean of a larger volume. This instrument simply registered the amount of time that the very tiny needle point was in a regime of vapor in relation to the time it was in contact with solid water (Ref. 1,2).



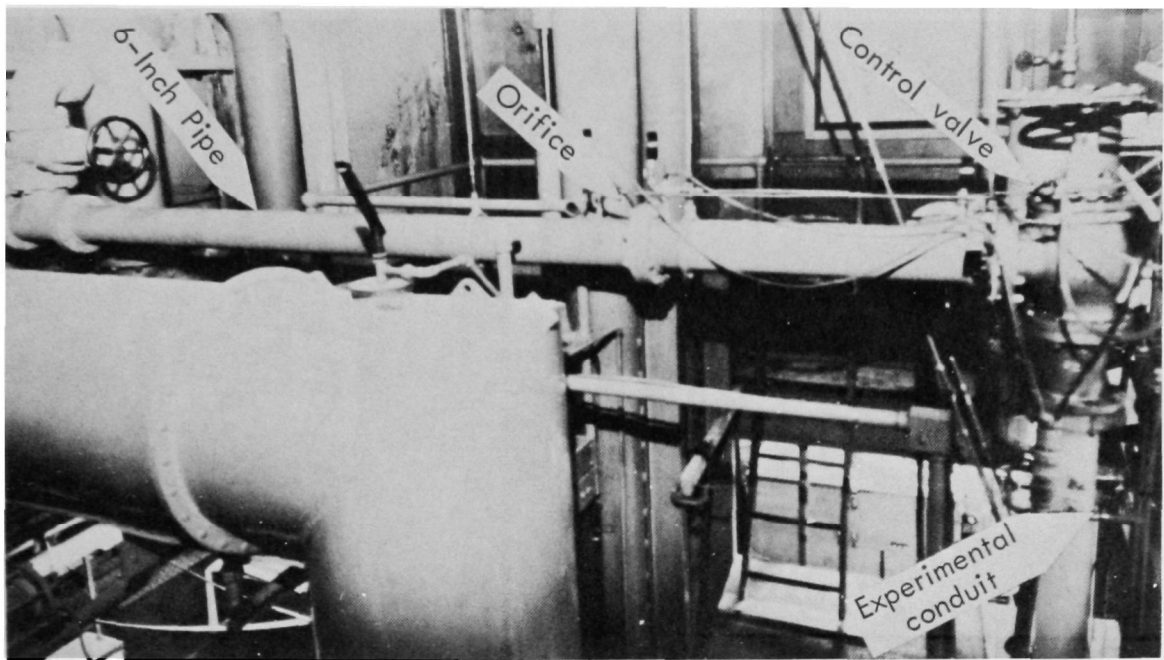


Fig. 2 - Inlet to Vertical Conduit showing Discharge Measuring Orifice and Control Valve

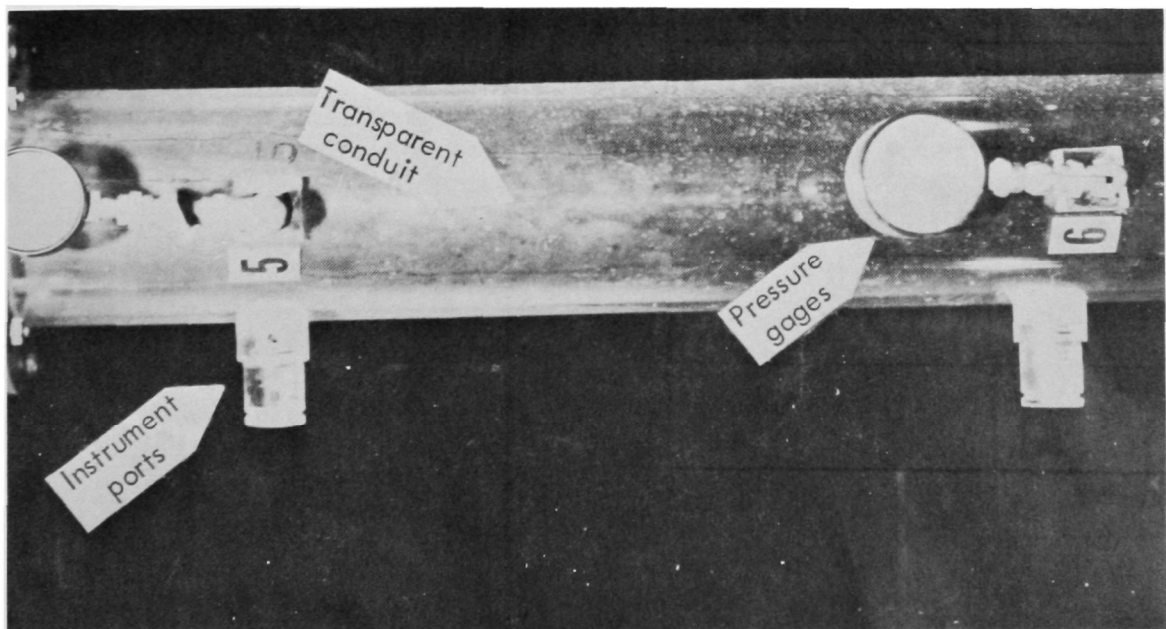


Fig. 3 - Transparent Experimental Vertical Conduit showing Pressure Gages and Instrument Ports

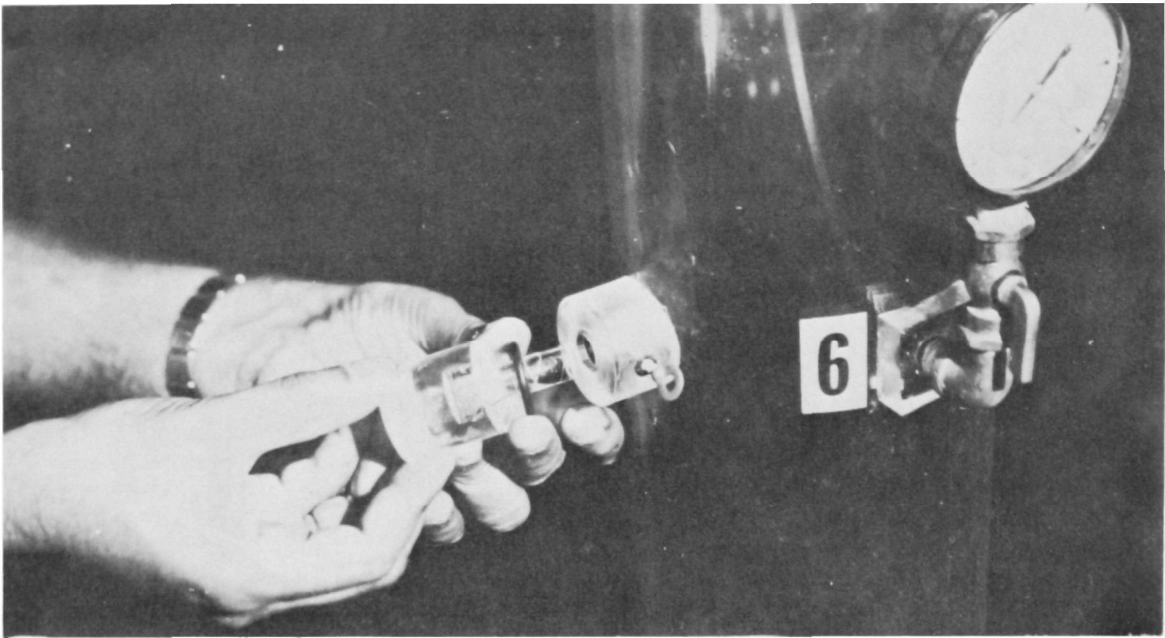


Fig. 4 - Detail of Instrument Ports for Vapor Concentration Measurements

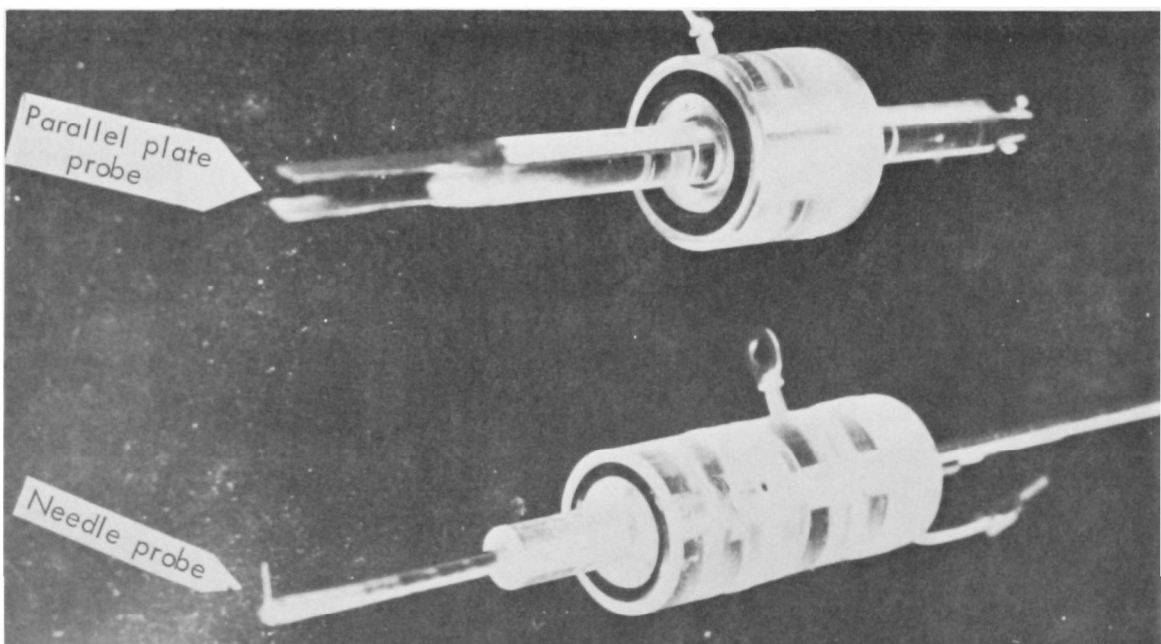


Fig 5 - Two types of Vapor-Concentration Sensors: (a) Parallel Plate Probe  
(b) Needle Probe



## SECTION V

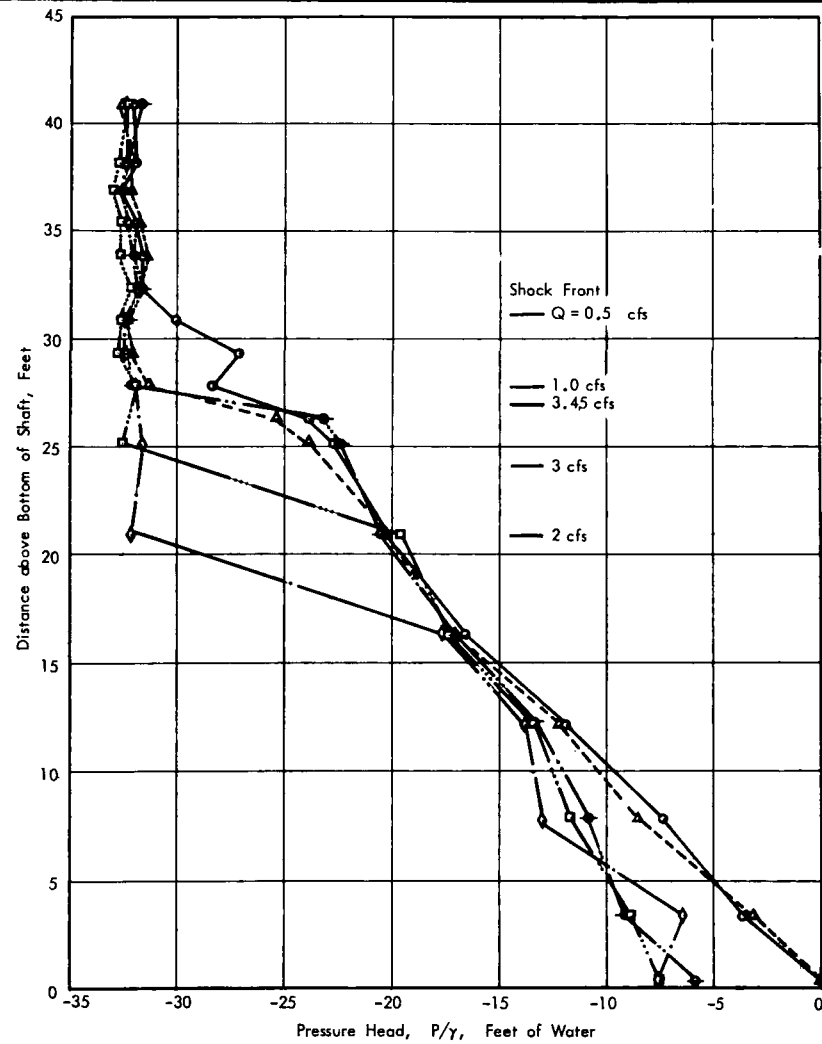
### EXPERIMENTAL RESULTS

#### Cavitation Studies

Measurements of the various flow properties are shown in Figs. 6 through 10. In Fig. 6, the pressure head,  $P/\gamma$ , has been plotted in terms of the elevation above the bottom of the conduit for various discharges through the system. Throughout the upper region--that is, above the shock front--and for all discharges the pressure is essentially constant at -31.75 ft of water. This is presumably the pressure at which cavitation occurs for the water being used in these experiments. The fact that this pressure is somewhat greater than the vapor pressure of pure water at this temperature is probably due to the dissolved air that is found in the natural river water. The figure also shows for each discharge a rather sudden increase in pressure as the shock is traversed and a relatively uniform rate of increase in the pressure gradient downstream of the shock front. These data have been replotted in Fig. 7 in terms of the piezometric head ( $P/\gamma + Z$ ) to develop the hydraulic gradient along the conduit. The plots show that the gradient in the upper region decreases linearly with the elevation and is the same for all discharges. At a particular elevation, which is a function of the discharge, there is a sudden increase in piezometric pressure across the shock front followed by a relatively flat gradient due to the frictional effects of the flow of the water phase through the lower regions of the conduit. The figure also gives some indication of the nature of the shock front, since for the smaller discharges (particularly 0.5 and 1.0 cfs) the hydraulic gradient shows a much more gradual transition to the solid water phase than the rather abrupt transition that occurs for the higher discharges.

In Fig. 8 longitudinal water-vapor concentration profiles have been plotted for various discharges, and the plot shows that the vapor concentration is reasonably constant upstream of the shock front and undergoes an abrupt reduction in the region of the shock front to relatively low values in the lower portions of the conduit. The concentration downstream of the shock front may, in fact, be air that was released above the shock front but which has not had time to be redissolved in the distance remaining below the shock front. The graph also shows that the vapor concentration above the shock front decreases systematically as the discharge increases. For a discharge of 0.5 cfs the mean concentration above the shock front is approximately 82 per cent, while that for a discharge of 3.65 cfs has been reduced to only 40 per cent. Below the shock front the air concentration is considerably less than the vapor concentration above the shock front and also decreases with the discharge.

One important result of these experiments is the delineation of the shock front that is observed when flow takes place down the conduit. Its elevation has been plotted in terms of the discharge in Fig. 9. For very small discharges the shock front occurs at an elevation roughly equivalent to the barometric height of the water; for increases in



## OPERATING CONDITIONS

1) Channel Water Level: El. 49.00

2) Water Temperature: 36°F

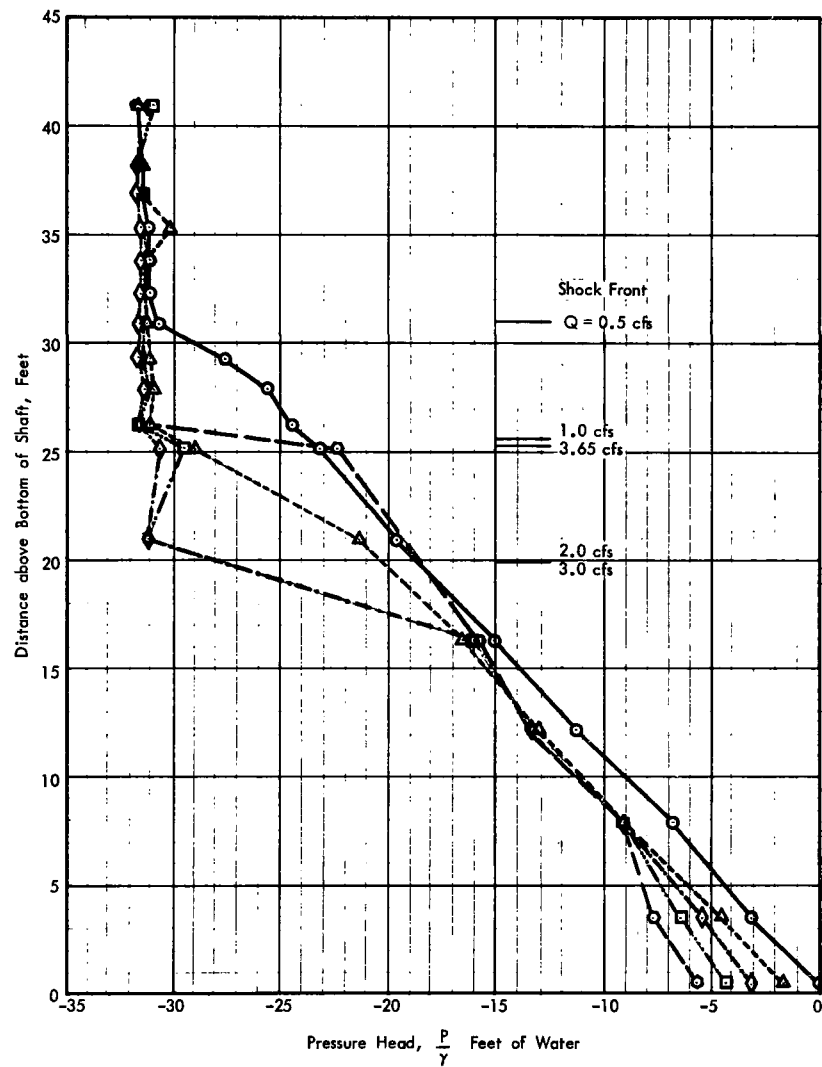
(Refer to Drwg. No. 1948492-2 for geometry.)

Symbol	Discharge, cfs
○	0.5
△	1.0
◇	2.0
□	3.0
⊕	3.45

Run Nos. 123, 119, 121(b), 122(b)  
Nov. 16, 23, 24, and 30, 1970

FIGURE 6a

STORM WATER DROP SHAFTS			
Federal Water Quality Administration			
PRESSURE HEAD VARIATION ALONG SHAFT			
SAINT ANTHONY FALLS HYDRAULIC LABORATORY			
UNIVERSITY OF MINNESOTA			
DRAWN	CSC	CHECKED	PPV
SCALE	Graphic	DATE	12-70
		NO.	1948492-11



## OPERATING CONDITIONS

- 1) Channel Water Level: El. 49.00
- 2) Water Temperature:  $\approx 80^{\circ}\text{F}$

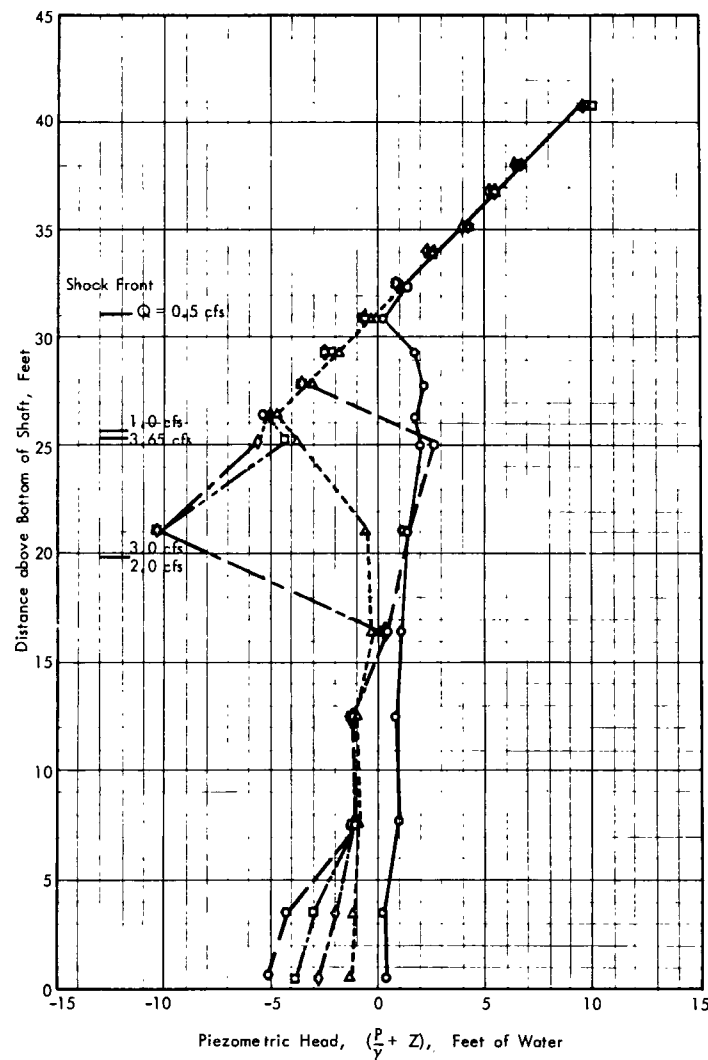
(Refer to Drwg. No. 1948492-2 for geometry.)

Symbol	Discharge in cfs
○	0.5
△	1.0
◇	2.0
□	3.0
⊙	3.65

June 29 and July 1, 1970

FIGURE 6b

STORM WATER DROP SHAFTS			
Federal Water Quality Administration			
PRESSURE HEAD VARIATION ALONG SHAFT			
SAINT ANTHONY FALLS HYDRAULIC LABORATORY			
UNIVERSITY OF MINNESOTA			
DRAWN DA	CHECKED PPV	APPROVED	
SCALE Graphic	DATE 12-70	NO. 1948492-6	



## OPERATING CONDITIONS

1) Channel Water Level: El. 49.00

2) Water Temperature:  $\approx 80^{\circ}\text{F}$ 

(Refer to Drwg. No. 1948492-2 for geometry.)

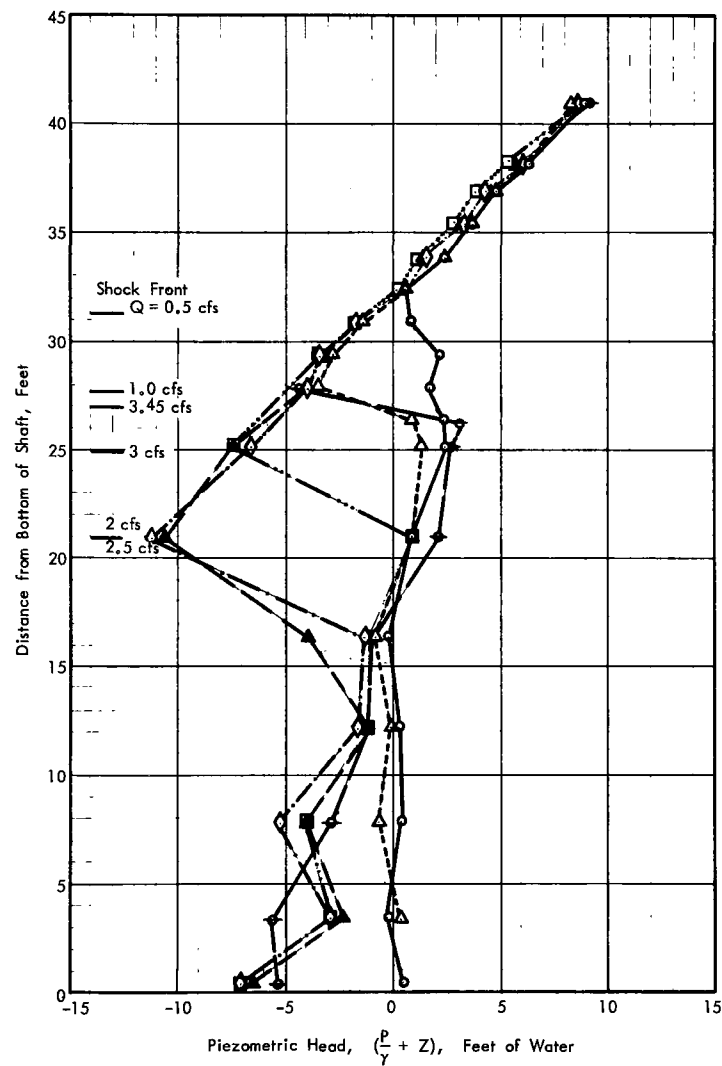
Symbol	Discharge in cfs
○	0.5
△	1.0
◇	2.0
□	3.0
○	3.65

FIGURE 7a

STORM WATER DROP SHAFTS  
Federal Water Quality Administration  
PIEZOMETRIC HEAD ALONG SHAFT

SAINT ANTHONY FALLS HYDRAULIC LABORATORY  
UNIVERSITY OF MINNESOTA

DRAWN DA	CHECKED PPV	APPROVED
SCALE Graphic	DATE 12-70	NO. 1948492-4



#### OPERATING CONDITIONS

1) Channel Water Level: El. 49.00

2) Water Temperature:  $\approx 36^{\circ}\text{F}$

(Refer to Drwg. No. 194B492-2 for geometry.)

Symbol	Discharge, cfs
○	0.5
△	1.0
◇	2.0
▲	2.5
□	3.0
⊕	3.45

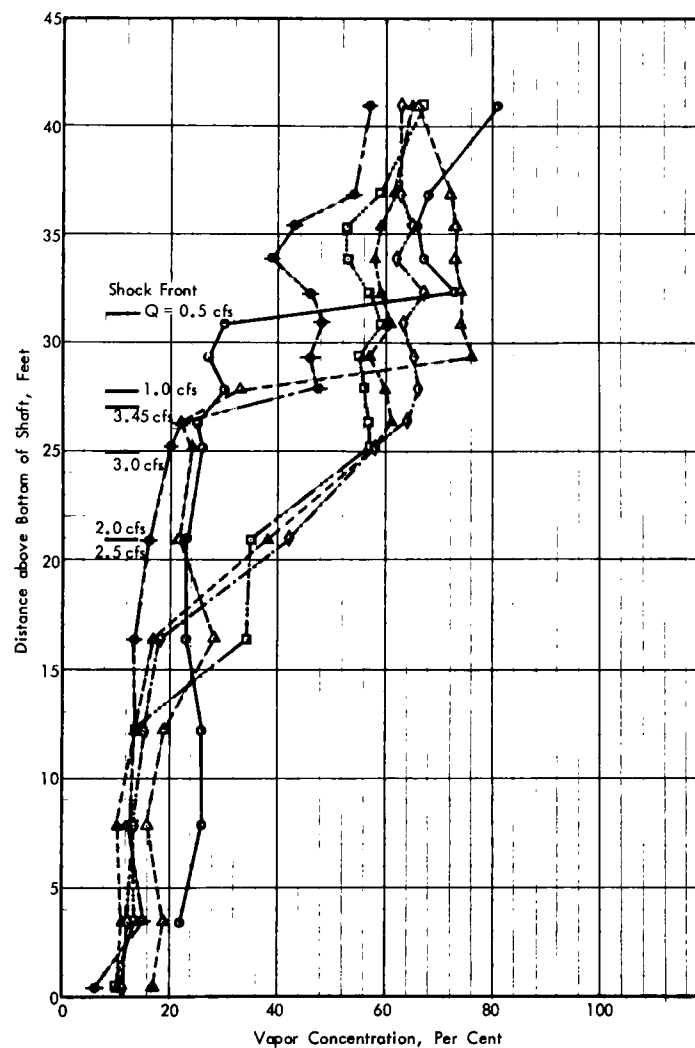
Run Nos. 122(a), 122(b), 123, 119  
Nov. 16, 23, 24, and 30, 1970

FIGURE 7b

STORM WATER DROP SHAFTS  
Federal Water Quality Administration  
PIEZOMETRIC HEAD ALONG SHAFT

SAINT ANTHONY FALLS HYDRAULIC LABORATORY  
UNIVERSITY OF MINNESOTA

DRAWN CSC	CHECKED PPV	APPROVED
SCALE 1" = 10'	DATE 12-70	NO. 194B492-12



OPERATING CONDITIONS

1) Channel Water Level: El. 49.00

2) Water Temperature:  $\approx 36^{\circ}\text{F}$

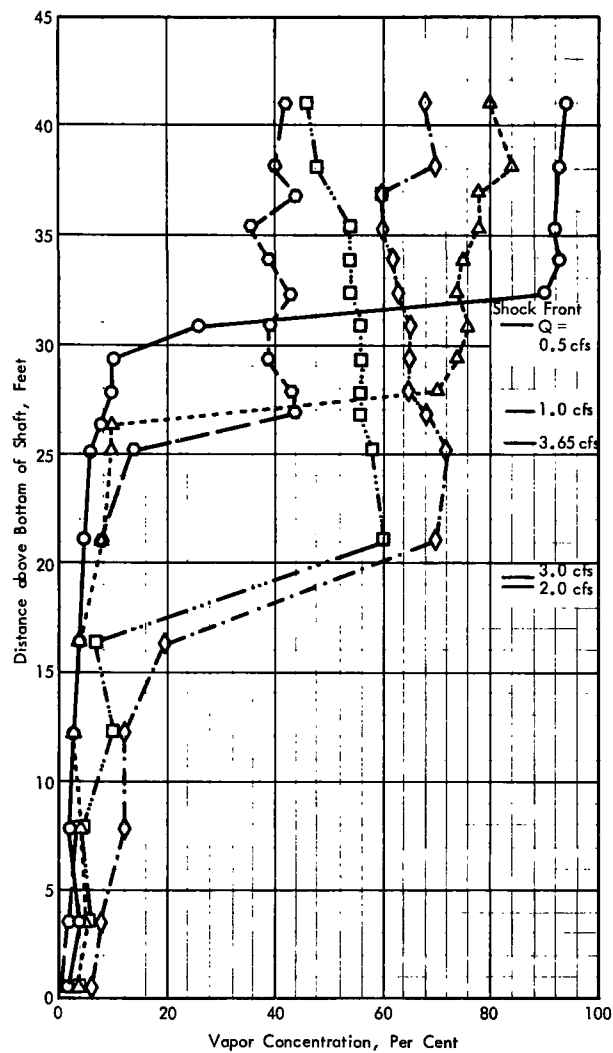
(Refer to Drwg. No. 194B492-2 for geometry.)

Symbol	Discharge, cfs
—○—	0.5
--△--	1.0
---◇---	2.0
--★--	2.5
---□---	3.0
--◆--	3.45

Run Nos. 119, 121(b), 122, 123  
Nov. 24, 23, 16, and 30, 1970

FIGURE 8a

STORM WATER DROP SHAFTS		
Federal Water Quality Administration		
VAPOR CONCENTRATIONS		
SAINT ANTHONY FALLS HYDRAULIC LABORATORY		
UNIVERSITY OF MINNESOTA		
DRAWN CSC	CHECKED PPV	APPROVED
SCALE Graphic	RATE 12-70	NO. 194B492-13



# OPERATING CONDITIONS

1) Channel Water Level: El. 49.00

2) Water Temperature:  $\approx 80^{\circ}\text{F}$

(Refer to Drwg. No. 1948492-2 for geometry.)

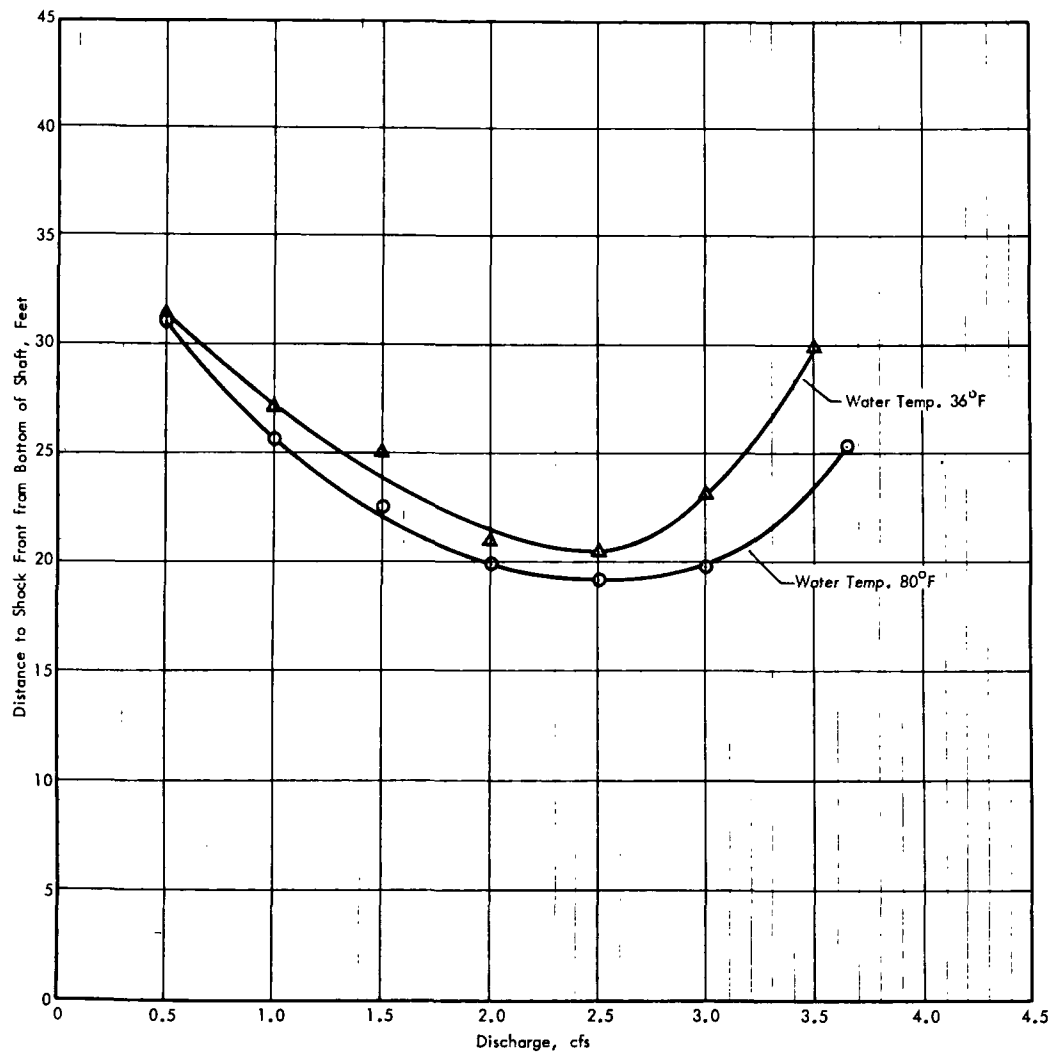
Symbol	Discharge in cfs
○	0.5
△	1.0
◇	2.0
□	3.0
○	3.65

August 25 thru 31, 1970

FIGURE 8b

STORM WATER DROP SHAFTS		
Federal Water Quality Administration		
VAPOR CONCENTRATIONS		
SAINT ANTHONY FALLS HYDRAULIC LABORATORY		
UNIVERSITY OF MINNESOTA		
DRAWN DA	CHECKED PPV	APPROVED
SCALE G	DATE 12-70	NO. 1948492-5





OPERATING CONDITIONS  
 Channel Water Level: El. 49.00  
 (Refer to Drwg. No. 1948492-2 for geometry.)

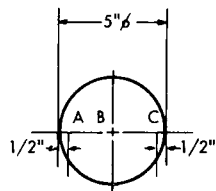
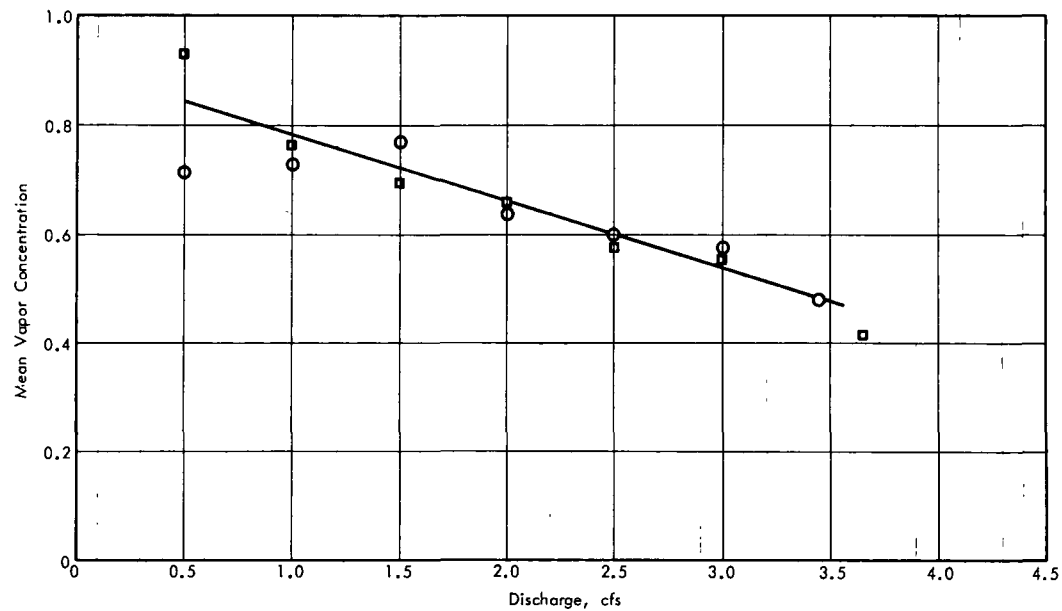
FIGURE 9

STORM WATER DROP SHAFTS		
Federal Water Quality Administration		
SHOCK-FRONT ELEVATION vs DISCHARGE		
SAINT ANTHONY FALLS HYDRAULIC LABORATORY UNIVERSITY OF MINNESOTA		
DRAWN DA	CHECKED PPV	APPROVED
SCALE Graphic	DATE 12-70	NO. 1948492-7

discharge the shock front elevation is lowered until it reaches a minimum at a discharge (in these experiments) of approximately 2.5 cfs. For discharges larger than this the shock front elevation again increases with increasing discharge. The maximum discharge obtainable in the present apparatus was 3.65 cfs, but it appears from the graph that if the discharge could have been increased above this value, the elevation of the shock front would also have risen further and would ultimately have reached the top of the conduit. In Fig. 10 the concentration of vapor in the region shows clearly that the vapor concentration, as suggested in Fig. 8, decreases with increasing discharge. It would appear from these two graphs that if the shock front were to reach the top of the conduit, so that the pipe flowed full, the vapor concentration would approach zero.

### Air Injection

The most apparent characteristic of the flow when atmospheric air is injected into the system is the immediate disappearance of the shock front and the development of a continuous hydraulic gradeline throughout the conduit. This is shown in Fig. 11, in which has been plotted the piezometric head ( $P/\gamma + Z$ ) with respect to elevation above the pipe outlet. These graphs do not show the discontinuities in pressure which are inherent in the flows in which cavitation occurs. The same effect is observed in the longitudinal air concentration profiles shown in Fig. 12. The air concentration tends toward constancy in the pipe below the point of injection. As would be expected for a constant rate of air injection, the air concentration is less for the higher water discharges than it is for the lower value. When a given water discharge is flowing through the system under a given gravitational head, the injection of air has the effect of reducing the water discharge. This is shown in Fig. 13, in which water discharge, again for a fixed total head, is plotted in terms of the rate of air flow injected into the system in pounds per second. Since the injection of a small quantity of air will effectively eliminate the shock front, it appears from Fig. 13 that this can be done with only a small reduction in the water discharge. This is perhaps shown more clearly in Fig. 14, in which the ratio of the air discharge to the water discharge, both in cfs, has been plotted in terms of the pressure at tap 5 (see Fig. 1) near the pipe inlet. All the data are grouped about a single curve and show that for small values of the ratio, the pressure at tap 5 is appreciably increased to a value well above the cavitation pressure for the flow.



NOTE: Observations of Concentrations relate to region above shock front and at location 'A' in sketch.

#### OPERATING CONDITIONS

Channel Water Level: El. 49.0±

(Refer to Drwg. No. 194B492-2 for geometry.)

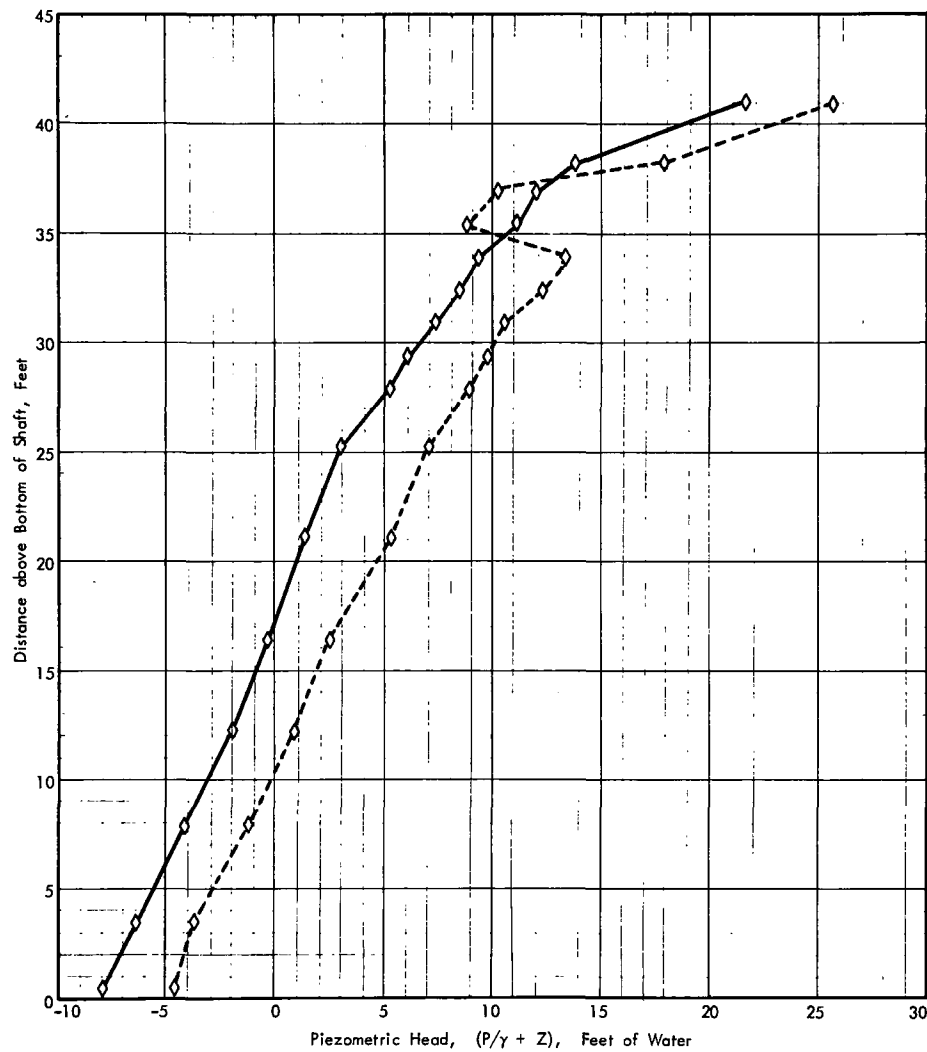
NOTE: Vapor Concentration =  $\frac{\text{Vol. of Vapor}}{\text{Vol. of Vapor} + \text{Vol. of Water}}$

Symbol	Temp °F
○	36
□	80

FIGURE 10

STORM WATER DROP SHAFTS  
Federal Water Quality Administration  
VAPOR CONCENTRATION vs DISCHARGE

SAINT ANTHONY FALLS HYDRAULIC LABORATORY UNIVERSITY OF MINNESOTA			
DRAWN	CSC	CHECKED	PPV
SCALE	Graphic	DATE	12-70
		APPROVED	NO. 194B492-8



## OPERATING CONDITIONS

1) Channel Water Level: El. 49.0

2) Water Temperature: 35°F

(Refer to Drwg. No. 194B492-2 for geometry)

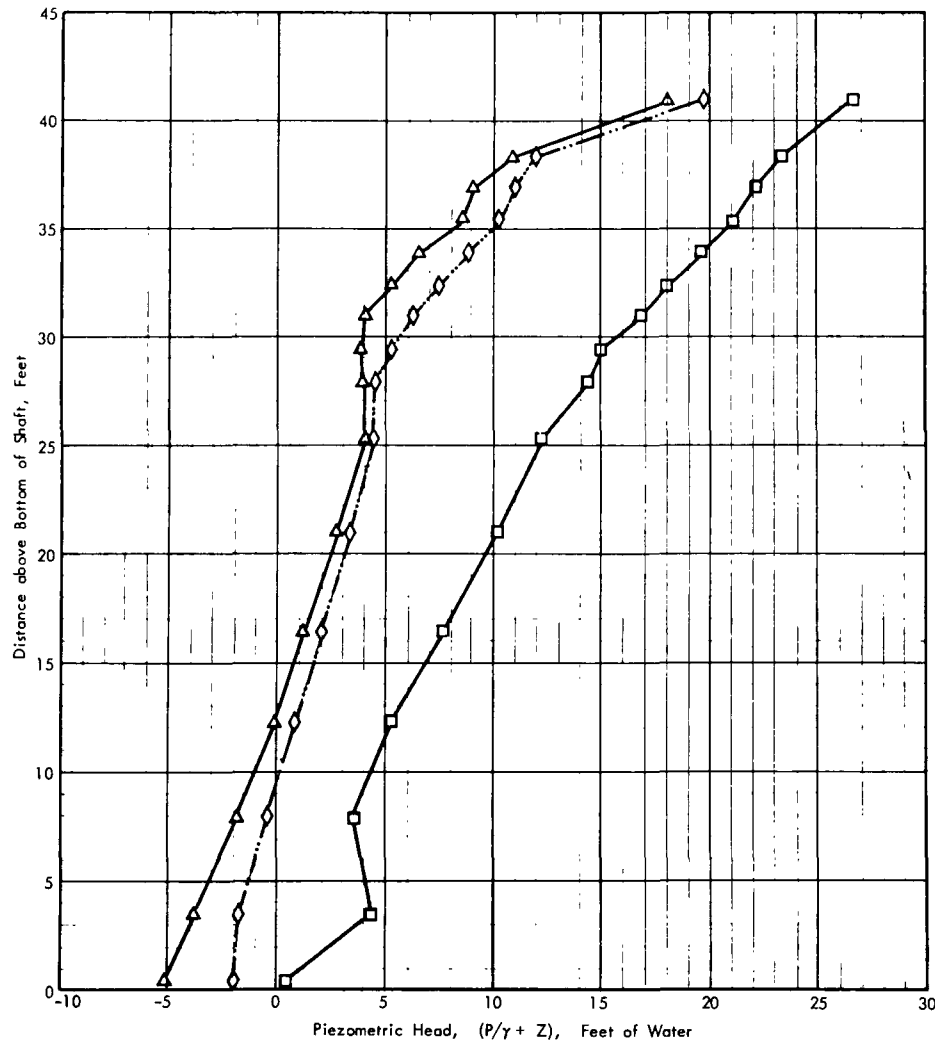
Symbol	Pressure		$Q_w$ cfs		$Q_a$		$\frac{Q_a}{Q_w}$	$\frac{Q_a}{Q_w + Q_a}$
	Reg psi	Tap #5 in Hg	No air	With air	lbs/sec	cfs	%	%
--◇--	17.5	-13.4	3	2.155	0.0761	1.76	81.7	44.9
—◇—	34	-17.1	2.5	2.08	0.0562	1.68	80.8	44.7

Note: Air injected through 4 equally spaced taps at El. 40.68

Run No. 200, Jan. 27, 1971

FIGURE 11a

STORM WATER DROP SHAFTS			
Federal Water Quality Administration			
PIEZOMETRIC HEAD ALONG SHAFT			
SAINT ANTHONY FALLS HYDRAULIC LABORATORY			
UNIVERSITY OF MINNESOTA			
DRAWN	CSC	CHECKED	CSC
SCALE	Graphic	DATE	Z-71
APPROVED			NO. 194B492-26



## OPERATING CONDITIONS

1) Channel Water Level: El. 49.00

2) Water Temperature:  $\approx 35^{\circ}\text{F}$ 

(Refer to Drwg. No. 1948492-2 for geometry)

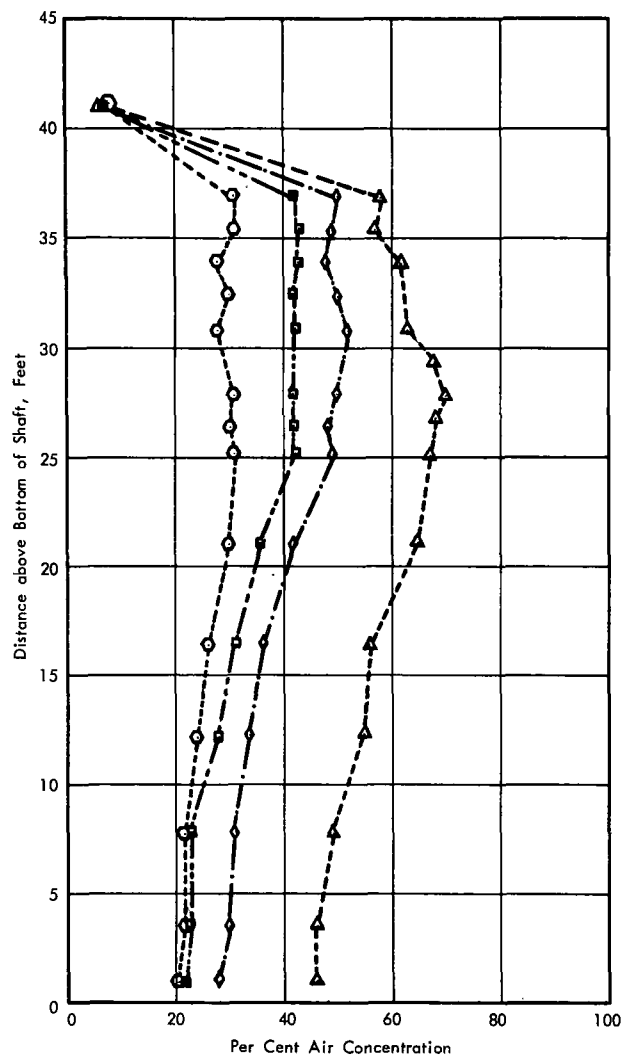
Symbol	Pressure		$Q_w$ cfs		$Q_a$		$\frac{Q_a}{Q_w}$	$\frac{Q_a}{Q_w + Q_a}$
	Reg psi	Tap #5 in Hg	No air	With air	lbs/sec	cfs	%	%
△	40	-23.9	3.65	3.2	0.0227	1.492	46.7	31.8
◇	20	-22.0	2.0	1.97	0.0242	1.20	60.9	37.9
□	20	-12.6	1.5	1.25	0.0516	1.13	90.4	47.5

Note: Air injected through 4 equally spaced taps at El. 40.68

Run No. 201, Feb. 1, 1971

FIGURE 11b

STORM WATER DROP SHAFTS		
Federal Water Quality Administration		
PIEZOMETRIC HEAD ALONG SHAFT		
SAINT ANTHONY FALLS HYDRAULIC LABORATORY		
UNIVERSITY OF MINNESOTA		
DRAWN CSC	CHECKED CSC	APPROVED
SCALE Graphic	DATE 2-71	NO. 1948492-28



# OPERATING CONDITIONS

Channel Water Level: El. 49.0

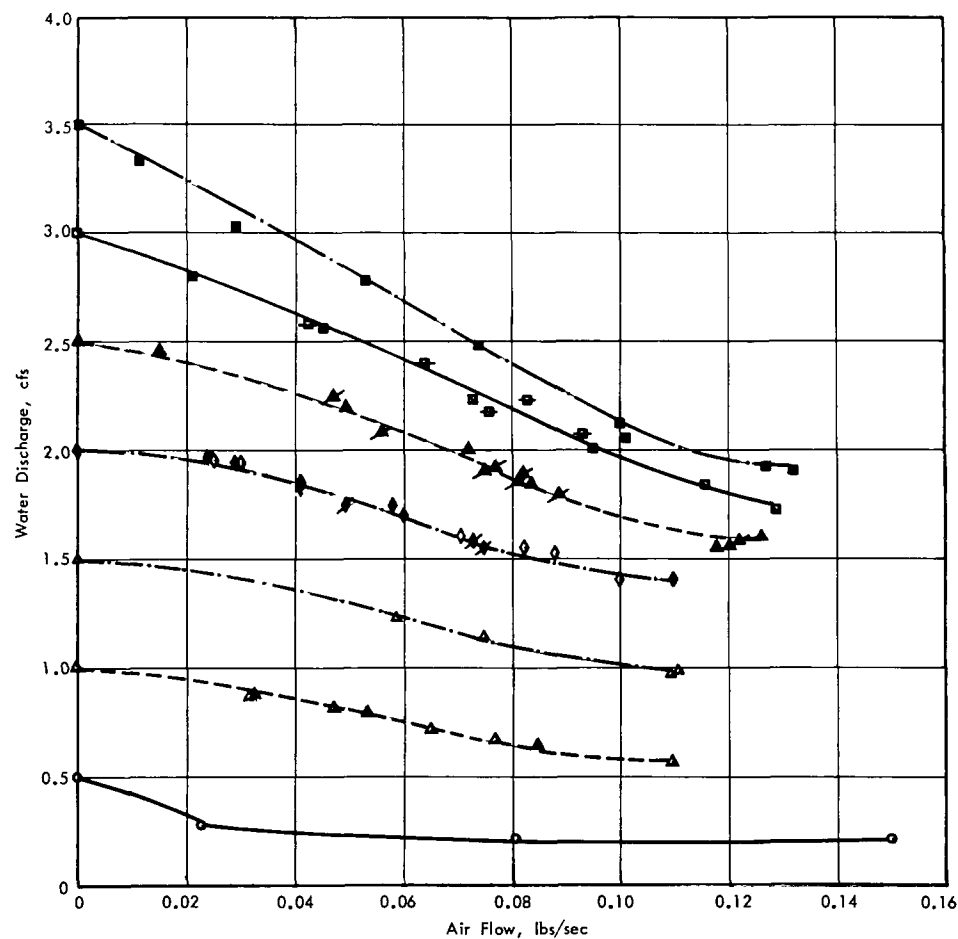
(Refer to Drwg. No. 1948492-2 for geometry)

Symbol	Water Discharge, cfs		Air Flow		Water Temp °F	Run No.	Date
	Before air injection	After air injection	lbs/sec	cfs			
—△—	1.0	0.78	0.0533	0.935	33.5	213	3-25-71
—◇—	2.0	1.86	0.0519	1.415	35	213	3-25-71
—■—	3.0	2.45	0.0544	1.855	35	213	3-25-71
—○—	3.65	2.7	0.0541	1.77	33.5	213	3-25-71

- Note: 1) Air flow in cfs calculated corresponding to pressure at Tap #5, 33.83 ft above shaft bottom
- 2) Air concentration measurements made at location A - Drwg. No. 1948492-8
- 3) Air injected through 4 equally spaced taps at El. 40.68

FIGURE 12

STORM WATER DROP SHAFTS			
Federal Water Quality Administration			
AIR CONCENTRATIONS ALONG SHAFT			
SAINT ANTHONY FALLS HYDRAULIC LABORATORY			
UNIVERSITY OF MINNESOTA			
DRAWN	PPV	CHECKED	PPV
SCALE	Graphic	DATE	3-71
APPROVED			NO. 1948492-29



## OPERATING CONDITIONS

Channel Water Level: El. 49.0

(Refer to Drwg. No. 1948492-2 for geometry)

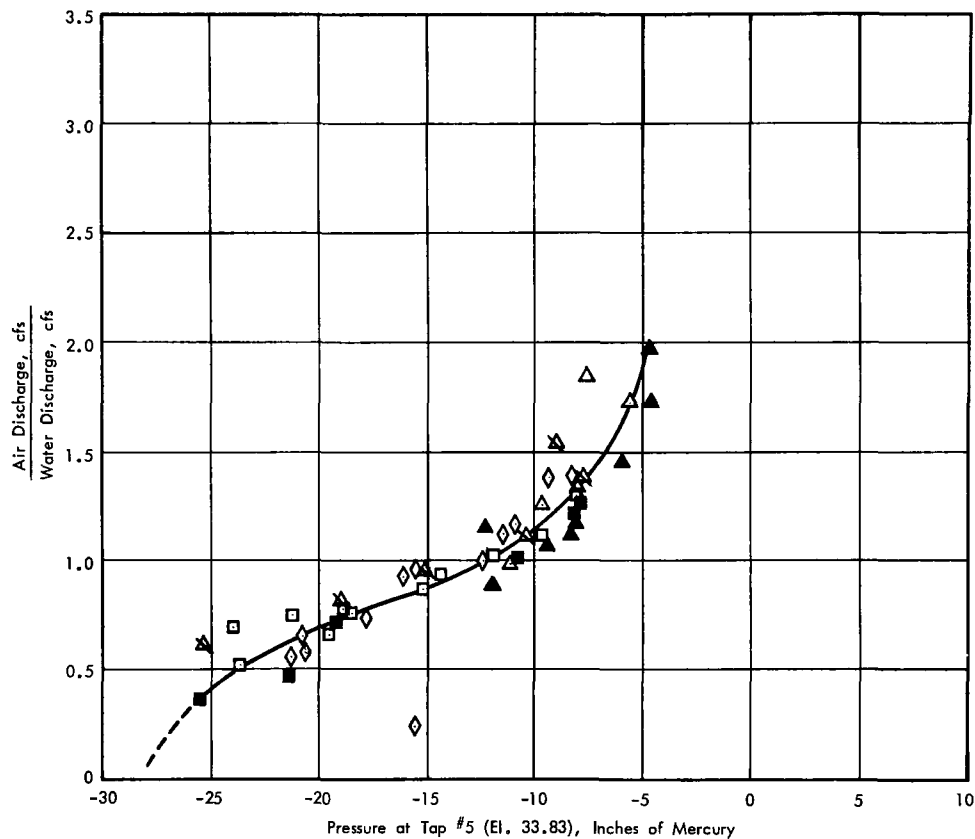
Symbol	Water Discharge (before air injection)	Water Temp °F	Run No.	Date
○—○	0.5	34	209	3-16-71
△—△	1.0	35	205	3-9-71
△—△	1.0	35	208	3-16-71
△—△	1.5	35	204	3-9-71
◇—◇	2.0	35	207	3-11-71
◇—◇	2.0	34	203	3-8-71
×—×	2.0	34	201	3-1-71
△—△	2.5	34	212	3-19-71
×—×	2.5	34	200	1-27-71
■—■	3.0	35	206	3-11-71
■—■	3.0	34	200	1-27-71
■—■	3.5	35	211	3-19-71

Note: Air injected through 4 equally spaced taps at El. 40.68

FIGURE 13

STORM WATER DROP SHAFTS		
Federal Water Quality Administration		
EFFECT OF AIR INJECTION ON WATER DISCHARGE		
SAINT ANTHONY FALLS HYDRAULIC LABORATORY UNIVERSITY OF MINNESOTA		
DRAWN M	CHECKED PPV	APPROVED
SCALE Graphic	DATE 3-71	NO. 1948492-31





#### OPERATING CONDITIONS

Channel Water Level: El. 49.00

(Refer to Drwg. No. 1948492-2 for geometry)

Symbol      Water Discharge, cfs  
(before air injection)

1.0

1.5

2.0

2.5

3.0

3.5

(Data of Run Nos. 202 through 213)

- Note: 1) Air injected through 4 equally spaced taps at El. 40.68
- 2) Air flow in cfs calculated corresponding to pressure at tap #5, 33.83 ft above shaft bottom

FIGURE 14

STORM WATER DROP SHAFTS		
Federal Water Quality Administration		
EFFECT OF AIR INJECTION ON SHAFT PRESSURE		
SAINT ANTHONY FALLS HYDRAULIC LABORATORY UNIVERSITY OF MINNESOTA		
DRAWN CSC	CHECKED CSC	APPROVED
SCALE 1"=10'	DATE 4-71	NO. 1948492-32

## SECTION VI

### ANALYSIS OF DATA

The experiments described above provide some insight into the mechanism by which cavitating flow may take place in a long vertical conduit. One can visualize three regions of flow. In the upper segment the flow of solid water is taking place in a receptacle of arbitrary shape (such as a sewer) with the prescribed free surface elevation. The water flows into the inlet of a long vertical conduit where the pressure is reduced to the cavitation pressure of the water if the depth of water over the conduit is sufficiently large to prevent air from being sucked into the flow. This condition can also be obtained if a valve exists in the system so that an appropriate head loss can be introduced to create a negative effective head. In the second region a mixture of water vapor and water droplets forms and continues to flow down the conduit at this constant cavitation pressure. The mixture may also contain a small amount of air released from solution in this region. In the third segment below the shock front the recondensed solid water flows down the pipe and discharges into the atmosphere. The pressures in this segment are considerably above the cavitation pressure. The water vapor in the air-water mixture must be recondensed at an elevation such that the piezometric pressure is greater than the atmospheric pressure at the end of the conduit. One can consider the overall phenomenon as being made up of a typical water flow in the upper supply channel and an essentially typical conduit flow at the lower end connected by a region of constant cavitation pressure in which a water-vapor mixture is flowing and whose length is determined by the overall length of the conduit and the discharge flowing through it. The cavitating segment serves, in effect, as the connecting link between the upper and lower water flows. On the basis of this somewhat simplified description one can develop a mathematical model which to some degree describes the flow (Refs. 3,4,5). Figure 15 is a diagrammatic sketch of a long vertical conduit through which water is flowing from an upper reservoir. Shown in the sketch are the free surface of the upper reservoir, the cavitation region between the inlet and the shock front, and the lower region in which essentially solid water is flowing.

One characteristic of the water vapor-water mixture in the cavitation region is the dramatic reduction in the velocity of sound. It has been shown (Ref. 6) that for such bubbly mixtures the sonic velocity can be expressed as

$$V_s = \left( \frac{P}{C(1-C)\rho_w} \right)^{1/2} \quad (1)$$

where  $V_s$  is the sonic velocity within the mixture,  $P$  is the absolute pressure of the medium,  $\rho_w$  is the density of the water, and  $C$  is the vapor concentration. This relationship, computed for the cavitation pressure, is shown in Fig. 16. The curve illustrates the generally low values of the sonic velocity over a wide range of vapor

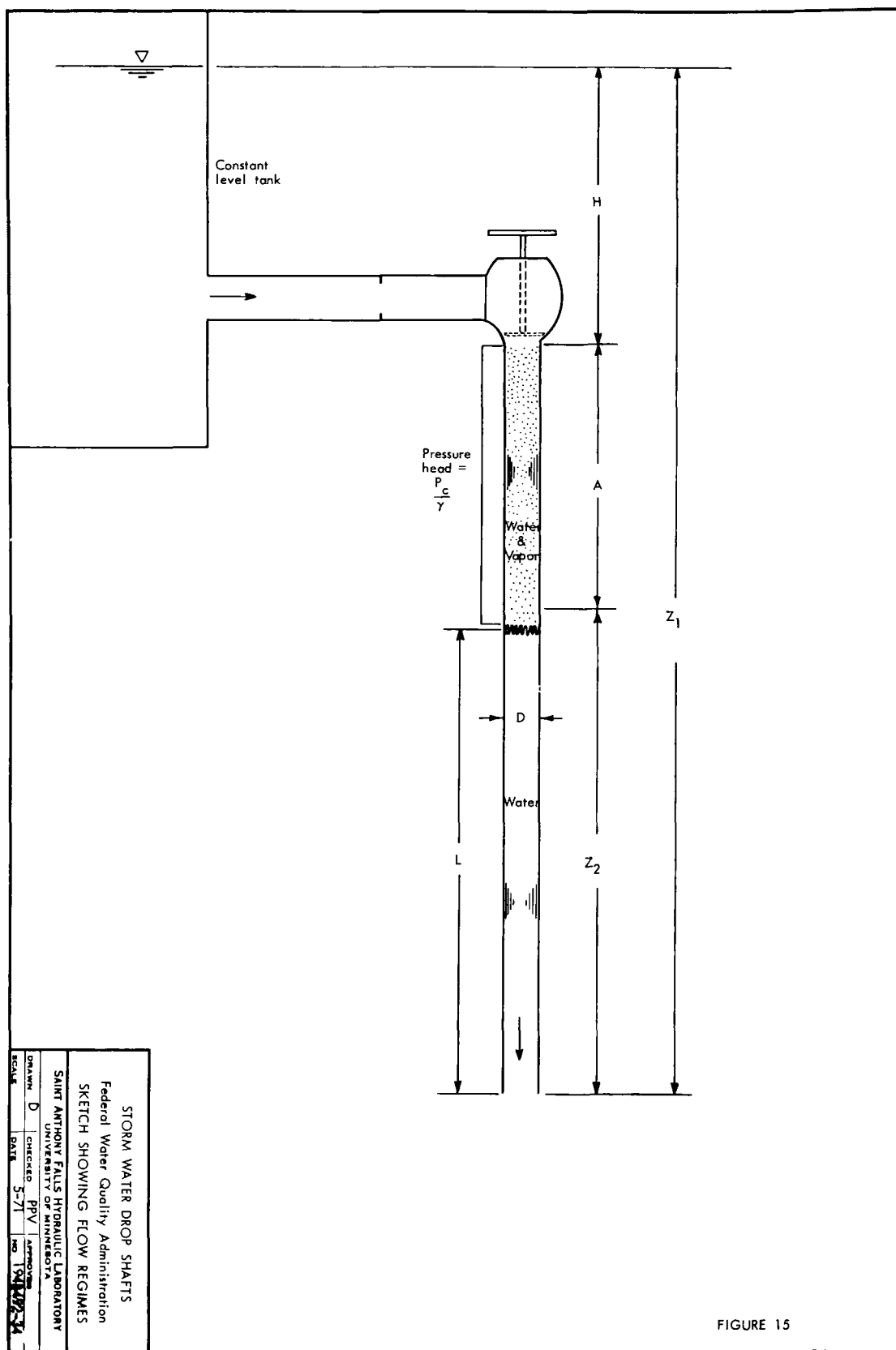
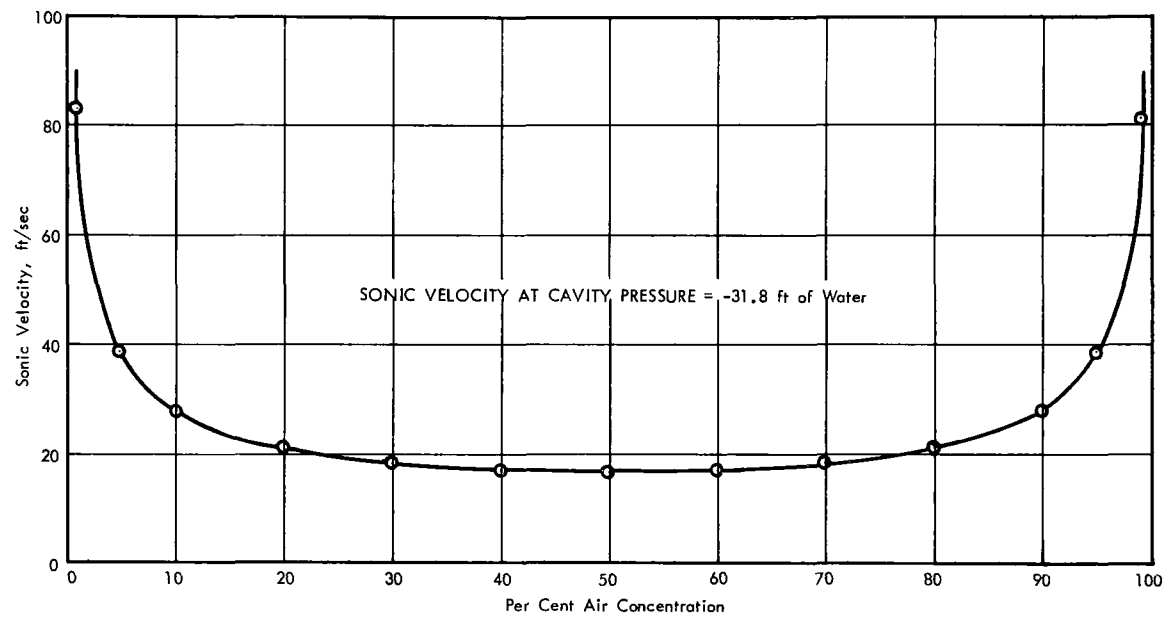


FIGURE 15



Sonic velocity calculated using  $V_s = \left[ \frac{P}{C(1-C)\rho_l} \right]^{1/2}$  where  $P$  = absolute pressure  
 $C$  = concentration of gas in the mixture by volume  
 $\rho_l$  = density of liquid

FIGURE 16

STORM WATER DROP SHAFTS			
Federal Water Quality Administration			
SONIC VELOCITY vs AIR CONCENTRATION			
SAINT ANTHONY FALLS HYDRAULIC LABORATORY			
UNIVERSITY OF MINNESOTA			
DRAWN	CSC	CHECKED	CSC
SCALE	Graphic	DATE	3-71
		APPROVED	NO. 194B492-33

concentrations. In addition, this sonic velocity is considerably lower than the mean velocity in the cavitation region, so that the flow is supersonic, and hence a shock front represents the transition to subsonic flow in the lower part of the conduit. When the vapor recondenses in the shock front, the sonic velocity increases rapidly, so that the flow downstream of the shock front is subsonic.

It is assumed that the mixture of vapor and water is homogeneous, that the velocity of the vapor is the same as that of the water, and that the temperature of the system remains constant. The energy balance, then, between the free water surface (point 1) and section 2 in the cavitation zone just above the shock front must include the energy required to vaporize the water in the cavity region. The energy balance between these two points can then be written as

$$\frac{V_1^2}{2} + h_1 + g Z_1 = \frac{V_2^2}{2} + h_2 + g Z_2 \quad (2)$$

where  $h_1 = (P_1/\rho_w) + u_1$  and  $h_2 = (P_2/\rho_2) + u_2$ . Here  $V_1$  and  $V_2$  are the velocities,  $h_1$  and  $h_2$  are the enthalpies, and  $Z_1$  and  $Z_2$  are the elevations at points 1 and 2, respectively;  $P_1$  and  $P_2$  are the pressures and  $u_1$  and  $u_2$  are the internal energies at points 1 and 2, respectively;  $g$  is the acceleration due to gravity;  $\rho_w$  is the density of water at point 1; and  $\rho_2$  is the density of the mixture of water and water vapor at point 2. At point 2 the enthalpy depends upon the enthalpy of both the water and the vapor. Let

$x$  = mass of vapor per unit mass of mixture

and  $1 - x$  = mass of water per unit mass of mixture

then

$$h_2 = xh_v + (1 - x)h_w = h_w + x(h_v - h_w) \quad (3)$$

but

$$h_w = \frac{P_2}{\rho_w} + u_w$$

so

$$h_2 = \left(\frac{P_2}{\rho_w} + u_w\right)_2 + x(h_v - h_w) \quad (4)$$

Then with substitution for the enthalpies, Eq. (2) can be written as

$$\frac{V_1^2}{2} + \frac{P_1}{\rho_w} + gZ_1 + u_1 = \frac{V_2^2}{2} + \frac{P_2}{\rho_w} + gZ_2 + u_2 + x(h_v - h_w) \quad (5)$$

The change in internal energy  $u_2 - u_1$  is due to friction on the boundary in the cavity region and to the friction, valves, orifice, and other obstructions in the inlet pipe, which can be lumped together as  $h_L$ . Then

$$u_2 - u_1 = f \frac{\Delta Z}{D} \frac{V_2^2}{2} + g h_L \quad (6)$$

where  $f$  is the effective Darcy friction factor for the cavitation region,  $h_L$  is the lumped head losses in the inlet conduit,  $D$  is the conduit diameter, and  $\Delta Z$  is the net length of conduit above point 2 over which frictional loss takes place. In addition, the mass vapor fraction can be expressed in terms of the volumetric concentration. If  $C$  is the volume of vapor per unit volume of water plus vapor, then by definition

$$x = \frac{\rho_v C}{\rho_w(1 - C) + \rho_v C} \approx \frac{\rho_v C}{\rho_w(1 - C)} \quad (7)$$

where  $\rho_v$  is the density of the water vapor. Further,

$$V_2 = \frac{Q_w}{A(1 - C)} = \frac{V_o}{1 - C} \quad (8)$$

where  $Q_w$  is the water discharge before cavitation and  $A$  is the cross-sectional area of the vertical conduit. The pressure at point 2 is the cavitation pressure--that is,

$$P_2 = P_c \quad (9)$$

Now substitution of Eqs. (6), (7), (8), and (9) into Eq. (5), and noting that  $V_1 = 0$ ,  $P_1 = 0$ , and  $V_o = Q/A$ , results in

$$Z_1 - Z_2 - \frac{P_c}{\gamma} = \frac{V_o^2}{2g(1 - C)^2} \left(1 + \frac{f\Delta Z}{D}\right) + \frac{C}{1 - C} \frac{\rho_v}{\rho_w} (h_v - h_w)J + h_L \quad (10)$$

where  $h_v$  and  $h_w$  now are in BTU/lb (in which units they can be obtained from steam tables) and  $J$  is the mechanical equivalent of the heat exchange. The vapor concentration in the cavity section can be computed from Eq. (10).

Utilizing the momentum equation and the equation of continuity through the shock front, the pressure downstream of the front can be written as

$$\frac{P_2}{\gamma} = \frac{P_c}{\gamma} + \frac{V_o^2}{g} \frac{C}{1-C} \quad (11)$$

Then the energy balance between section 3 downstream of the shock front and the pipe outlet can be written as

$$\frac{P_c}{\gamma} + \frac{V_o^2}{g} \left( \frac{C}{1-C} \right) + L = \frac{f'L}{D} \cdot \frac{V_o^2}{2g} \quad (12)$$

so that the elevation of the shock front referred to the pipe outlet becomes

$$L = \frac{\frac{P_c}{\gamma} + \frac{V_o^2}{g} \left( \frac{C}{1-C} \right)}{\left( \frac{f'}{D} \frac{V_o^2}{2g} - 1 \right)} \quad (13)$$

In Eq. (13) all the terms are known, since  $P_c/\gamma = -31.75$  ft or the vapor pressure of the water,  $V_o = Q/A$  where  $Q$  is the water discharge and  $A$  is the cross-sectional area of the conduit whose diameter is  $D$ ,  $C$  is computed from Eq. (10), and  $f'$  is the friction factor for the conduit.

The calculated elevation of the shock front in terms of the discharge and the experimental geometry has been plotted in Fig. 17. In these computations it was assumed that the friction factor for the flow of the water-vapor mixture in the cavitation zone was negligible for all discharges below that which corresponded to the minimum value of the shock front elevation. For discharges above this point the friction factor was linearly increased to that corresponding to the maximum discharge. The experimental data for the shock front elevation in terms of discharge are also plotted in Fig. 17 for comparison. The experiments indicated that above the minimum the elevation of the shock front tended to increase until for a certain discharge it would presumably reach the conduit inlet and the entire system would run full. This is also indicated by Eq. (13), which gives the discharge for which the shock front has reached the top of the pipe. Any further increase in



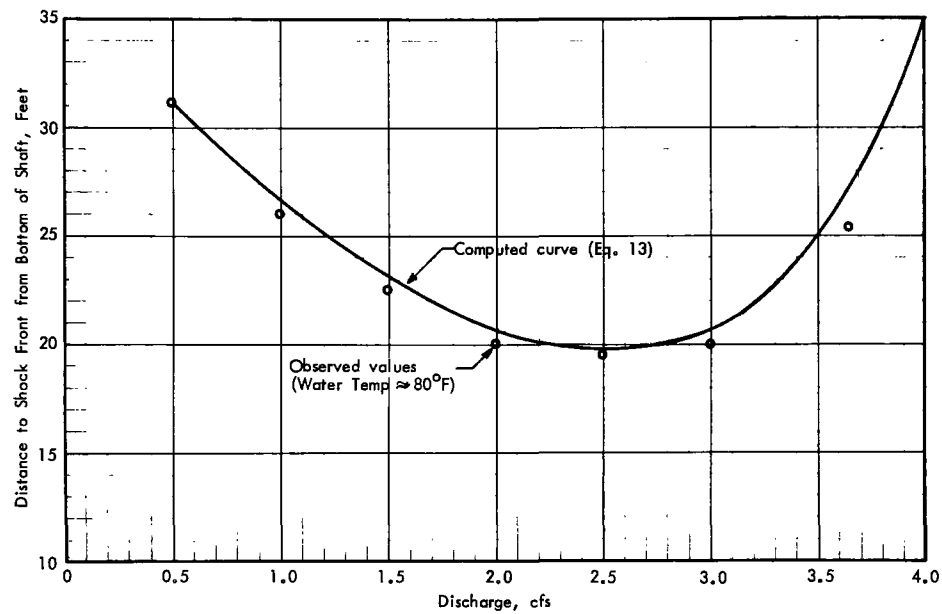


FIGURE 17

STORM WATER DROP SHAFTS		
Federal Water Quality Administration		
COMPUTED AND OBSERVED SHOCKFRONT ELEVATIONS		
SAINT ANTHONY FALLS HYDRAULIC LABORATORY UNIVERSITY OF MINNESOTA		
DRAWN CSC	CHECKED CSC	APPROVED
SCALE Graphic	DATE 5-71	NO. 1948492-38

discharge requires a corresponding increase in total head. Figure 17 shows that with the proper choice of constants in the equations, reasonable agreement can be obtained between experimental and computed results.

In Fig. 18 the experimental values of the vapor concentration in the cavitating region have been plotted in terms of the discharge for comparison with the computed relationship. Here the experimental values of the concentration follow the same trend as is indicated by the theoretical computations and show that as the discharge increases toward the maximum, the vapor concentration decreases and approaches zero.

The experimental results and the analysis based upon these results show that as the discharge increases, the elevation of the shock front also increases until the conduit runs full. The relatively short (42 ft) hydraulic model upon which these experiments were made was not comparable in length to the vertical drop shafts which would represent the prototype. Therefore, utilizing the relationship developed above, the results were extrapolated to conduits of the same size and roughness, but of greatly increased length such as is found in practice. Figure 19 shows the theoretical elevation of the shock front for various discharges and conduit lengths for a constant net head. These computations show that the elevation of the shock front rises very rapidly for small increases in discharge as full flow is approached. This suggests that the shock front may lose its identity in an almost instantaneous condensation of the water vapor to solid water throughout the remaining pipe length as the maximum discharge is approached. In addition, the curves for different conduit lengths tend to separate as the minimum shock front elevation is approached. All the curves tend toward the elevation corresponding to that of a water column for zero discharge.

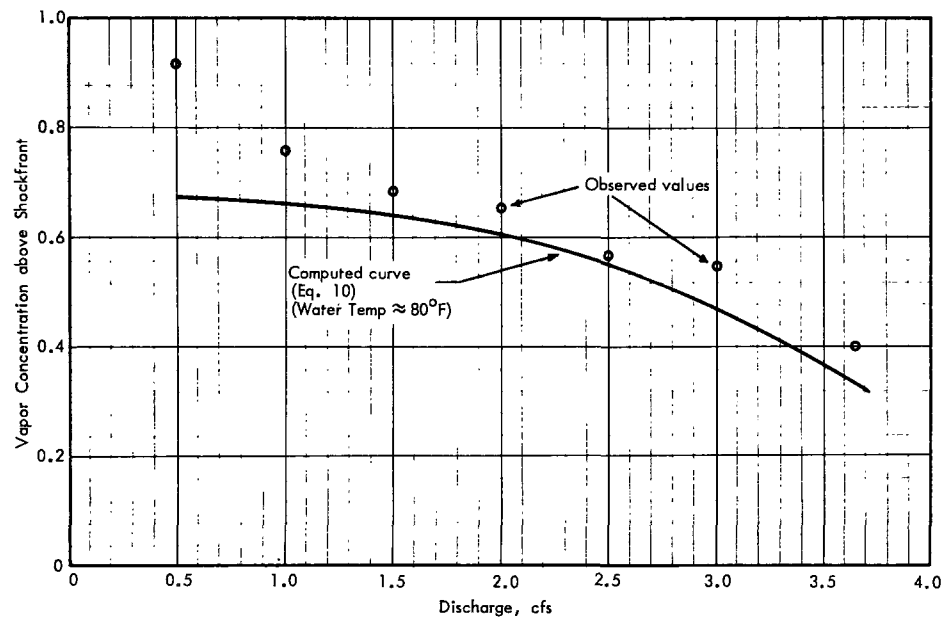
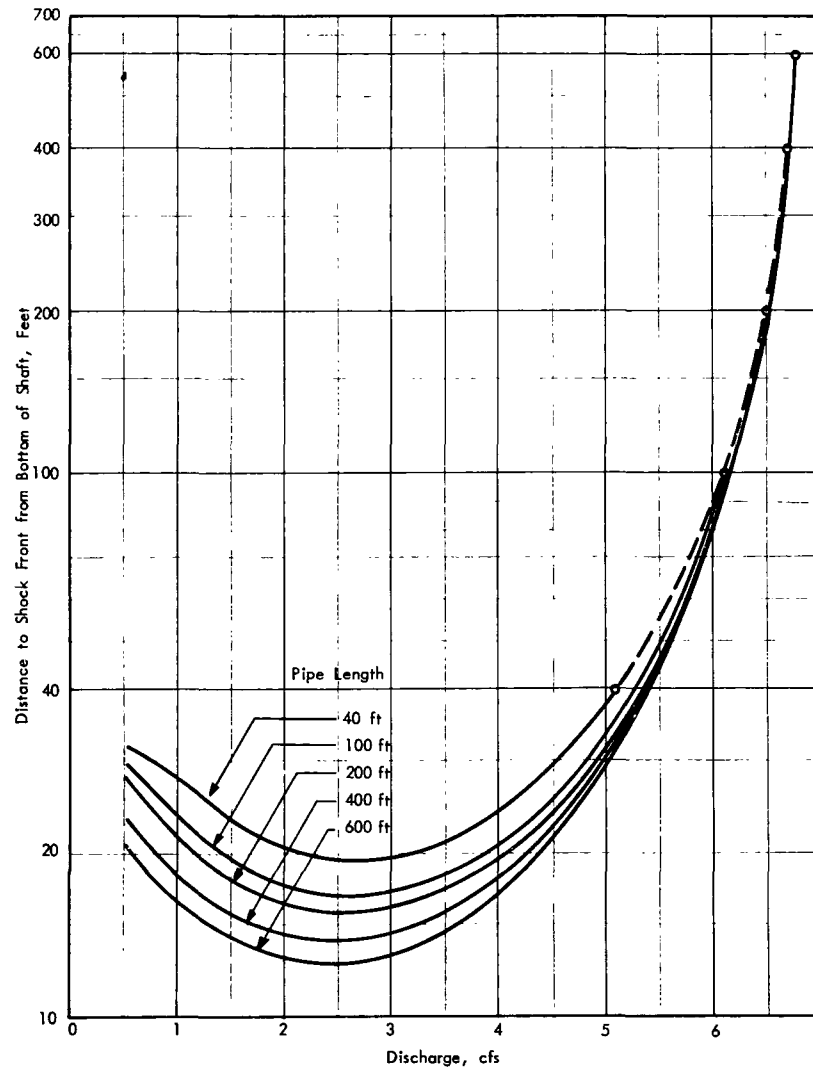


FIGURE 18

STORM WATER DROP SHAFTS Federal Water Quality Administration			
COMPUTED AND OBSERVED VAPOR CONCENTRATIONS ABOVE SHOCKFRONT			
SAINT ANTHONY FALLS HYDRAULIC LABORATORY UNIVERSITY OF MINNESOTA			
DRAWN D	CHECKED PPV	APPROVED	
SCALE Graphic	DATE 5-71	NO. 1948492-39	



NOTE:

- 1) Calculations based on Eqs. (10) and (13)
- 2) Pipe diameter: 5 inches
- 3) Water temperature: 80°F

FIGURE 19

STORM WATER DROP SHAFTS		
Federal Water Quality Administration		
THEORETICAL CURVES showing SHOCKFRONT ELEVATION for VARYING PIPE LENGTHS		
SAINT ANTHONY FALLS HYDRAULIC LABORATORY		
UNIVERSITY OF MINNESOTA		
DRAWN D	CHECKED PPV	APPROVED
SCALE Graphic	DATE 5-71	NO. 1948492-40

## SECTION VII

### HEAD DISCHARGE RATING CURVES

Although the experimental studies dealt primarily with the cavitation regime for flow in long vertical culverts, it is appropriate to consider this regime in relation to the complete head-discharge rating curve for the system. The nature of the flow, including the existence of cavitation flow, depends upon the interaction between the head, the discharge, and the conduit length, diameter, roughness, and inlet geometry. In a particular drop shaft system a number of flow regimes can be visualized. When the discharge is sufficiently large, the conduit may flow full without cavitation. If the conduit is very long, the flow may cavitate in the upper regions. If there is a valve in the inlet system and the conduit is long enough, it can be made to cavitate for relatively low discharges. For an open system--that is, one without a control valve--the system may act as an orifice or weir in which air is insufflated into the conduit through the upper pool. The head-discharge curves can be plotted on a single chart so that the several flow regimes can be delineated (Refs. 7,8).

#### Transitional Flow

Transitional flow is restricted to the so-called open systems: vertical conduits which are open to the atmosphere at the inlet and have no intervening flow control device such as a valve. In such a system the vertical conduit is connected directly to the bottom of the supply channel or sewer. Initially, for very low discharges, the water will trickle over the edge of the conduit like flow over a weir. As the discharge increases, the jets over the edge will become large enough to meet in the pipe and effectively seal the inlet so that the flow approximates that through a horizontal orifice. Below the inlet, however, the flow will tend to fill the conduit with water or at least a dense spray. As more of the pipe is filled, the pressure in the region below the inlet will decrease below the atmospheric pressure in accordance with the Bernoulli principle. This pressure difference will increase and ultimately break the surface and permit air to be insufflated through the inlet and into the conduit. As the discharge increases, the head over the inlet will increase and the pressure in the region below the inlet will tend to decrease still more, since there will be a successively greater opportunity for the downflowing water to fill the conduit. This situation can be described by the equation

$$\frac{Q}{D^{5/2}} = \left[ \frac{\pi^2 g}{8} \left( \frac{H}{D} - \frac{P_2}{\gamma D} \right) \right]^{1/2} = 6.3 \left( \frac{H}{D} - \frac{P_2}{\gamma D} \right)^{1/2} \quad (14)$$

where  $Q/D^{5/2}$  is a semi-dimensionless discharge since the constant  $(g)^{1/2}$  has been transposed,  $H$  is the head over the inlet,  $D$  is the conduit diameter, and  $P_2/\gamma$  is the pressure head just below the inlet. For low values of  $H/D$ ,  $P_2/\gamma$  approaches zero and the flow

approaches that through an orifice. As the discharge increases,  $H$  increases and  $P_2/\gamma$  decreases until air is insufflated. The minimum value of  $P_2/\gamma$  is  $P_c/\gamma = -31.75$  ft when the flow in the conduit cavitates. For a given head the pressure head  $P_2/\gamma$  also depends upon the geometry of the inlet and the flow pattern in the supply channel. For purposes of illustration, the head-discharge curve for a weir in the form

$$\frac{Q}{D^{5/2}} = 10.27 \left(\frac{H}{D}\right)^{3/2} \quad (15)$$

has been plotted in Figs. 20, 21, and 22 and labeled "weir flow." A wide band of uncertainty has been sketched on either side of this curve in the region where the head is positive. It is recognized that the flow in this transitional region is not a weir flow, but the pressures given by Eq. (14) are typical of those that might be expected for such heads and discharges.

### Cavitation Flow

In the experiments described earlier it was found that when the flow in the upper part of the conduit was cavitating, the pressure was constant throughout the cavitating region at a value of  $P_2/\gamma = P_c/\gamma = -31.75$  ft.

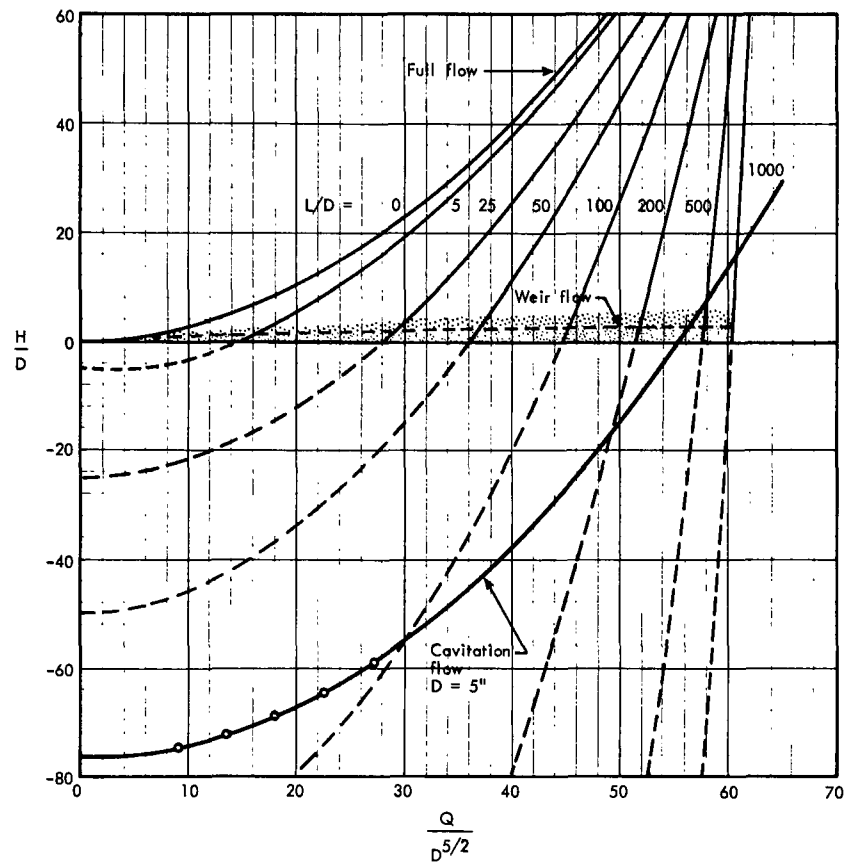
In those experiments, however, the flow took place in a closed system--i.e., one in which the total head  $H_T$  was constant and the flow was controlled by a valve which introduced the appropriate headloss into the system. The valve permitted the net head to be negative so that cavitating flow could be generated. In this case the net head  $H$  is the total head above the top of the vertical conduit minus the headloss in the valve and associated piping, or

$$H = H_T - h_L \quad (16)$$

in which  $h_L$  may be larger than  $H_T$ , giving rise to negative net heads. Experiments showed that as the discharge increased, the elevation of the shock front also increased and tended to fill the pipe. Assuming that just at the instant when the pipe ran full the pressure head was still approximately  $-31.75$  ft, the head-discharge relation could be described by Eq. (14) with  $P_2/\gamma$  replaced by  $P_c/\gamma$ , the cavitation pressure. Then

$$\frac{Q}{D^{5/2}} = 6.3 \left( \frac{H}{D} + \frac{31.75}{D} \right)^{1/2} \quad (17)$$

It will be noted that in this case the head-discharge relationship depends upon the absolute value of  $D$ , and a separate curve will be developed for each conduit diameter. To show the effect of conduit

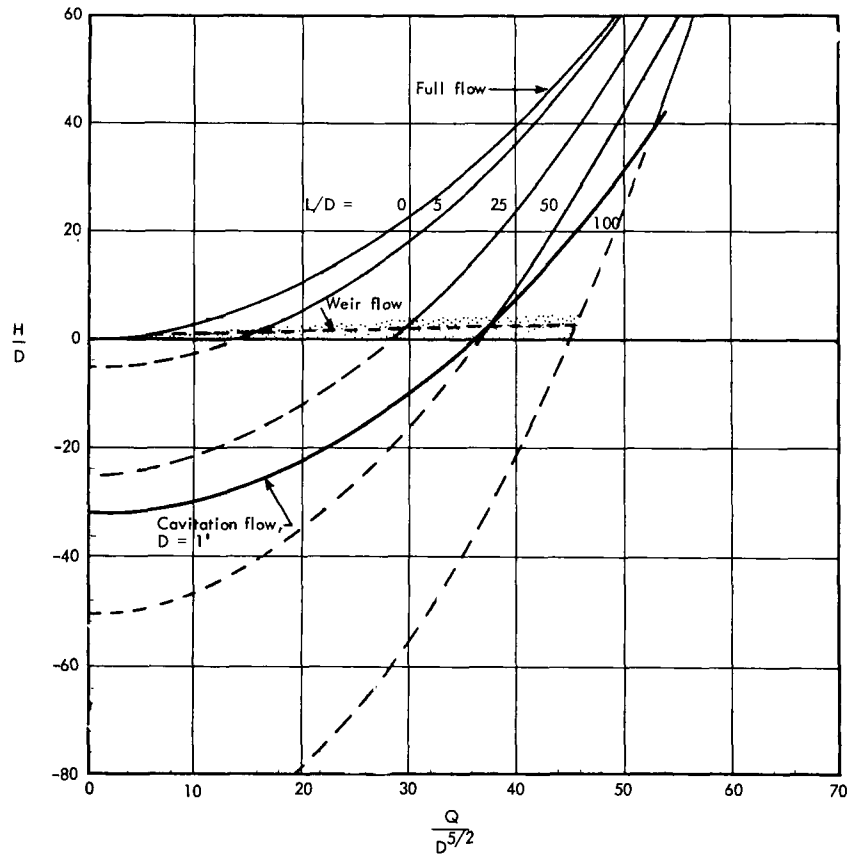


## FLOW REGIME EQUATIONS

1. Weir flow:  $\frac{Q}{D^{5/2}} = 10.27 \left( \frac{H}{D} \right)^{3/2}$
2. Cavitation flow:  $\frac{Q}{D^{5/2}} = 6.3 \left( \frac{H}{D} - \frac{P_o}{D} \right)^{1/2}$
3. Full flow:  $\frac{Q}{D^{5/2}} = 6.3 \left( \frac{\frac{H}{D} + \frac{L_o}{D}}{1 + f \frac{L_o}{D}} \right)^{1/2}$   
 $f = 0.01$  (assumed)

FIGURE 20

STORM WATER DROP SHAFTS		
Federal Water Quality Administration		
DISCHARGE RATING CURVES - Dia. = 5.0 in.		
SAINT ANTHONY FALLS HYDRAULIC LABORATORY		
UNIVERSITY OF MINNESOTA		
DRAWN D	CHECKED PPV	APPROVED
SCALE Graphic	DATE 5-71	NO. 1948492-35



## FLOW REGIME EQUATIONS

1. Weir flow:  $\frac{Q}{D^{5/2}} = 10.27 \left( \frac{H}{D} \right)^{3/2}$

2. Cavitation flow:  $\frac{Q}{D^{5/2}} = 6.3 \left( \frac{H}{D} - \frac{P_o/\gamma}{D} \right)^{1/2}$

3. Full flow:  $\frac{Q}{D^{5/2}} = 6.3 \left( \frac{\frac{H}{D} + \frac{L_o}{D}}{1 + f \frac{L_o}{D}} \right)^{1/2}$   
 $f = 0.01$  (assumed)

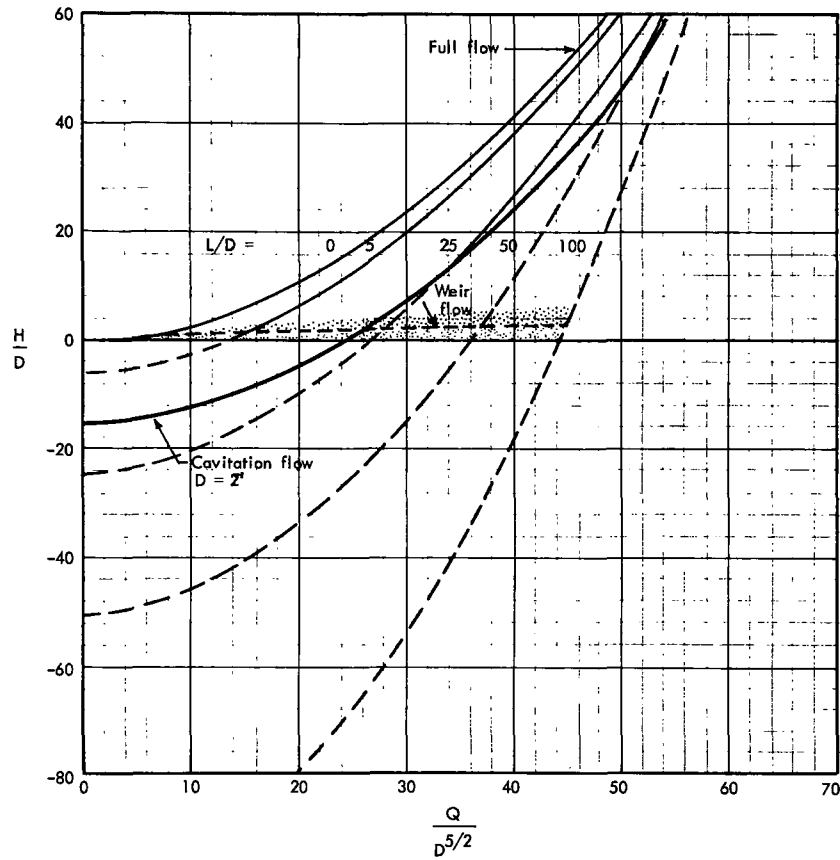
FIGURE 21

STORM WATER DROP SHAFTS  
 Federal Water Quality Administration  
 DISCHARGE RATING CURVES - Dia. = 1.0 ft

SAINT ANTHONY FALLS HYDRAULIC LABORATORY  
 UNIVERSITY OF MINNESOTA

DRAWN D	CHECKED PPV	APPROVED
SCALE Graphic	DATE 5-71	NO. 194B492-36





# FLOW REGIME EQUATIONS

1. Weir flow:  $\frac{Q}{D^{5/2}} = 10.27 \left( \frac{H}{D} \right)^{3/2}$

2. Cavitation flow:  $\frac{Q}{D^{5/2}} = 6.3 \left( \frac{H}{D} - \frac{P_o/\gamma}{D} \right)^{1/2}$

3. Full flow:  $\frac{Q}{D^{5/2}} = 6.3 \left( \frac{\frac{H}{D} + \frac{L_o}{D}}{1 + f \frac{L_o}{D}} \right)^{1/2}$   
 $f = 0.01$  (assumed)

FIGURE 22

STORM WATER DROP SHAFTS		
Federal Water Quality Administration		
DISCHARGE RATING CURVES - Dia. = 2.0 ft		
SAINT ANTHONY FALLS HYDRAULIC LABORATORY		
UNIVERSITY OF MINNESOTA		
DRAWN D	CHECKED PPV	APPROVED
SCALE Graphic	DATE 5-71	NO. 1948492-37

diameter on the rating curves, computations were made for a 5 in. conduit such as was used in the experimental program (Fig. 20), a 1 ft diameter drop shaft (Fig. 21) and a 2 ft diameter drop shaft (Fig. 22). These individual curves have been labeled "cavitation flow" on the graphs. It is apparent from Eq. (17) and the respective plots that the larger the conduit, the larger is the relative head for cavitation flow.

Further, as the relative discharge  $Q/D^{5/2}$  increases, the relative head,  $H/D$ , required for cavitation also increases. That portion of the curve lying below the abscissa  $H/D = 0$  applies to a closed system, while the portion above the curve applies to either system.

### Full Flow

As the discharge for cavitating flow increases, the elevation of the shock front also increases until ultimately the conduit is running full. The discharge for which this occurs will depend upon the length of the conduit as well as on its diameter and roughness. Curves can be plotted to show the head-discharge relationship for various pipe lengths. Application of the Bernoulli equation between the inlet and the outlet results in

$$\frac{Q}{D^{5/2}} = 6.3 \left( \frac{\frac{H}{D} + \frac{L_o}{D}}{1 + \frac{f' L_o}{D}} \right)^{1/2} \quad (18)$$

where in addition to the terms previously defined,  $L_o$  is the length of the conduit and  $f'$  is the Darcy friction factor for the conduit. It is apparent from Eq. (18) that a separate head-discharge curve will result for each  $L_o/D$  value. A set of such curves for typical  $L_o/D$  ratios from zero to 1000 has been plotted on each of Figs. 20, 21, and 22. On the graphs these lines intersect the curves for transitional flow and cavitation flow and thus show how the several flow transitions take place.

### Flow Behavior Patterns

The curves in Figs. 20, 21, and 22 show the behavior patterns for three conduits of different diameters. The graphs differ only in the position of the cavitation flow curve, which shifts along with the conduit diameter. Figure 20 has been drawn for the 5 in. experimental conduit. This was a closed system, since a valve was used to initiate cavitation for relatively low discharges. The region covered by the experiments is shown by the experimental points plotted at the lower end of the cavitation flow curve.

In a closed or valve-controlled system such as that used in the experimental program, the path followed by the head-discharge relationship can be traced by considering the various curves. Assume that initially the discharge is zero; then the head is zero and the point starts at the

origin. If the valve is initially open a small amount, the point will move along the so-called "weir flow" curve until the valve takes control and no more air is insufflated into the conduit. At this point cavitation will occur and the head-discharge point will drop to the cavitation flow curve with a significantly negative net relative head. As the valve is opened to increase the discharge, the point follows the cavitation flow curve until it intersects the full flow curve having the appropriate length-diameter ratio,  $L_0/D$ . At this intersection the point follows the full flow curve until the maximum discharge is reached. If, as for short conduits, the full flow curve does not intersect the cavitation flow curve, the head-diameter ratio  $H/D$  will fall only to the full flow curve and the conduit will immediately run full without cavitating. For very long conduits the point may follow the cavitation flow curve until  $H/D$  becomes positive before the conduit flows full.

In an open system, since  $h_L$  is negligible, the net head will never become negative. In this case the head-discharge locus follows along the transitional curve labeled "weir flow" until it intersects the appropriate curve for full flow. It then moves up the full flow curve to the maximum value. However, if the conduit is very long and the head available is adequate, the head-discharge locus moves along the weir flow curve until it intersects the cavitation flow curve, along which it then moves until it reaches the appropriate full flow curve.

It appears that a variety of flow patterns are available, depending upon the geometry of the system. This variety provides the designer with several possibilities for developing a system within the constraints imposed by external conditions.

Better curves can be drawn with respect to a particular installation so that the head can be determined more accurately, but the graphs in these figures indicate the nature of flow in long vertical conduits and can be used to describe the flow qualitatively.

## SECTION VIII

### ACKNOWLEDGMENTS

This research project was conducted by the St. Anthony Falls Hydraulic Laboratory, University of Minnesota, Prof. Edward Silberman, director. Prof. Alvin G. Anderson, principal investigator, directed the project and also wrote the report. Mr. P. P. Vaidyaraman, graduate research assistant, performed the experiments with the assistance of Mr. Chung Sang Chu, research assistant. The apparatus and some of the instrumentation were constructed in the laboratory shops, of which Mr. Frank R. Dressel is the superintendent. Mrs. Shirley Kii prepared the manuscript.

The project was sponsored by the Water Quality Office of the Environmental Protection Agency, and Mr. Clarence C. Oster was Project Officer.

## SECTION IX

### REFERENCES

1. Lamb, O. P. and Killen, J. M., An Electrical Method of Measuring Air Concentration in Flowing Air-Water Mixtures, Technical Paper No. 2-B, St. Anthony Falls Hydraulic Laboratory, University of Minnesota, March 1950.
2. Neal, L. G. and Bankoff, S. G., "A High Resolution Resistivity Probe for Determination of Local Void Properties in Gas-Liquid Flow," AIChE Journal, July 1963.
3. Griebe, R. W.; Winter, E. R. F.; and Schoenhals, R. J., Two-Phase Flow in Vibrating Discharge Lines, Final Report, Part III, School of Mechanical Engineering, Purdue University, Lafayette, Indiana, July 1968.
4. Eddington, R. B., Investigation of Supersonic Shock Phenomena in a Two-Phase (Liquid-Gas) Tunnel, Technical Paper No. 32-1096, Jet Propulsion Laboratory, Pasadena, California, March 1967.
5. Wallis, G. B., One-Dimensional Two-Phase Flow, McGraw-Hill Book Company, New York, 1969.
6. Schiebe, F. R.; Wetzel, J. M.; and Foerster, K. E., Studies of Flow Characteristics of a Compressible Bubbly Mixture about Supercavitating Bodies in a Converging-Diverging Nozzle, Technical Paper No. 48-B, St. Anthony Falls Hydraulic Laboratory, University of Minnesota, April 1964.
7. Blaisdell, F. W., Hydraulics of Closed Conduit Spillways - Part I - Theory and Its Applications, Technical Paper No. 12-B, St. Anthony Falls Hydraulic Laboratory, University of Minnesota, February 1958.
8. Straub, L. G.; Anderson, A. G.; and Bowers, C. E., Effect of Inlet Design on Capacity of Culverts on Steep Slopes, Project Report No. 37, St. Anthony Falls Hydraulic Laboratory, University of Minnesota, April 1954.

## SECTION X

### GLOSSARY OF SYMBOLS

- A = Area of pipe,  $\text{ft}^2$
- C = Vapor concentration by volume
- D = Diameter of pipe, ft
- f = Darcy friction factor for the cavitating portion of the pipe
- f' = Darcy friction factor for the pipe
- g = Acceleration due to gravity,  $\text{ft}/\text{sec}^2$
- H = Head at inlet to pipe, ft
- h = Enthalpy, BTU/lb
- $h_L$  = Headloss, ft
- J = Conversion factor, 778 ft-lb/BTU
- L = Distance to shock front from bottom of shaft, ft
- $L_O$  = Overall length of pipe, ft
- P = Pressure,  $\text{lbs}/\text{ft}^2$
- $P/\gamma$  = Pressure head, ft of water
- $P_c/\gamma$  = Cavitation pressure, ft of water
- Q = Discharge, cfs
- u = Internal energy, BTU/lb
- V = Velocity, ft/sec
- $V_O$  = Bulk velocity =  $Q_w/A$ , ft/sec
- $V_s$  = Sonic velocity, ft/sec
- x = Vapor quality
- Z = Elevation above datum, ft
- $\rho$  = Density,  $\text{slugs}/\text{ft}^3$
- $\gamma$  = Specific weight,  $\text{lbs}/\text{ft}^3$

#### Subscripts:

a = air          v = vapor          w = water

<b>1</b>	Accession Number  <b>W</b>	<b>2</b>	Subject Field & Group  Ø8A	<b>SELECTED WATER RESOURCES ABSTRACTS</b> INPUT TRANSACTION FORM
<b>5</b>	Organization Minnesota Univ., Minneapolis, St. Anthony Falls Hydraulic Lab.			
<b>6</b>	Title HYDRAULICS OF LONG VERTICAL CONDUITS AND ASSOCIATED CAVITATION			
<b>10</b>	Author(s) Anderson, A. G. Vaidyaraman, P. P. Chu, C. S.	<b>16</b>	Project Designation EPA, WQO Contract No. 14-12-861 Project Number 11034 FLU	
		<b>21</b>	Note	
<b>22</b>	Citation			
<b>23</b>	Descriptors (Starred First) *Drains, *Sewers, *Cavitation, Air Entrainment, Closed Conduits			
<b>25</b>	Identifiers (Starred First) *Dropshafts, *Cavitation Flow, Pressure Conduits			
<b>27</b>	Abstract <p>Experimental studies have been undertaken to examine the flow in long vertical conduits with particular reference to the design of storm water drop shafts. A distinguishing characteristic of such flow is the cavitation regime which may exist in the head-discharge relationship. The cavitation regime will develop when the conduit is sufficiently long and the head sufficiently large. It can also be generated at a lower head if a control valve is installed in the supply line so that the net head can be negative. The cavitation region consists of a rather finely divided mixture of water and water vapor at a constant cavitation pressure of about -32.0 ft of water throughout the region and for all discharges. The concentration of vapor, while relatively constant throughout the cavitation region, decreases with increasing discharge. The location of the shock front is also a function of the discharge.</p> <p>If a small amount of air is introduced into the system, the cavitation region is eliminated, the pressure gradient is more uniform, and the flow consists of a white mixture of air and water.</p> <p>The study also showed that the cavitation region is only one phase of the total head-discharge regime and that its existence depends upon the design of the structure. (Anderson-Minnesota)</p>			
Abstractor	Alvin G. Anderson	Institution	St. Anthony Falls Hydr. Lab., U. of Minn., Minneapolis	

Continued from inside front cover....

11022 --- 08/67	Phase I - Feasibility of a Periodic Flushing System for Combined Sewer Cleaning
11023 --- 09/67	Demonstrate Feasibility of the Use of Ultrasonic Filtration in Treating the Overflows from Combined and/or Storm Sewers
11020 --- 12/67	Problems of Combined Sewer Facilities and Overflows, 1967 (WP-20-11)
11023 --- 05/68	Feasibility of a Stabilization-Retention Basin in Lake Erie at Cleveland, Ohio
11031 --- 08/68	The Beneficial Use of Storm Water
11030 DNS 01/69	Water Pollution Aspects of Urban Runoff, (WP-20-15)
11020 DIH 06/69	Improved Sealants for Infiltration Control, (WP-20-18)
11020 DES 06/69	Selected Urban Storm Water Runoff Abstracts, (WP-20-21)
11020 --- 06/69	Sewer Infiltration Reduction by Zone Pumping, (DAST-9)
11020 EXV 07/69	Strainer/Filter Treatment of Combined Sewer Overflows, (WP-20-16)
11020 DIG 08/69	Polymers for Sewer Flow Control, (WP-20-22)
11023 DPI 08/69	Rapid-Flow Filter for Sewer Overflows
11020 DGZ 10/69	Design of a Combined Sewer Fluidic Regulator, (DAST-13)
11020 EKO 10/69	Combined Sewer Separation Using Pressure Sewers, (ORD-4)
11020 --- 10/69	Crazed Resin Filtration of Combined Sewer Overflows, (DAST-4)
11024 FKN 11/69	Stream Pollution and Abatement from Combined Sewer Overflows - Bucyrus, Ohio, (DAST-32)
11020 DWF 12/69	Control of Pollution by Underwater Storage
11000 --- 01/70	Storm and Combined Sewer Demonstration Projects - January 1970
11020 FKI 01/70	Dissolved Air Flotation Treatment of Combined Sewer Overflows, (WP-20-17)
11024 DOK 02/70	Proposed Combined Sewer Control by Electrode Potential
11023 FDD 03/70	Rotary Vibratory Fine Screening of Combined Sewer Overflows, (DAST-5)
11024 DMS 05/70	Engineering Investigation of Sewer Overflow Problem - Roanoke, Virginia
11023 EVO 06/70	Microstraining and Disinfection of Combined Sewer Overflows
11024 --- 06/70	Combined Sewer Overflow Abatement Technology
11034 FKL 07/70	Storm Water Pollution from Urban Land Activity
11022 DMU 07/70	Combined Sewer Regulator Overflow Facilities
11024 EJC 07/70	Selected Urban Storm Water Abstracts, July 1968 - June 1970
11020 --- 08/70	Combined Sewer Overflow Seminar Papers
11022 DMU 08/70	Combined Sewer Regulation and Management - A Manual of Practice
11023 --- 08/70	Retention Basin Control of Combined Sewer Overflows
11023 FIX 08/70	Conceptual Engineering Report - Kingman Lake Project
11024 EXF 08/70	Combined Sewer Overflow Abatement Alternatives - Washington, D.C.